NEUTRINO MASSES AND THE LHC: TESTING TYPE II SEESAW

Pavel Fileviez Pérez[1],[*] Tao Han [1,2],[†] Guiyu Huang [1],[‡] Tong Li [1,3],[§] and Kai Wang [1][¶]

[1] *Department of Physics, University of Wisconsin, Madison, WI 53706, USA*

[2] *KITP, University of California, Santa Barbara, CA 93107, USA*

[3] *Department of Physics, Nankai University, Tianjin 300071, P.R. China*

(Dated: October 30, 2018)

We demonstrate how to systematically test a well-motivated mechanism for neutrino mass generation (Type-II seesaw) at the LHC, in which a Higgs triplet is introduced. In the optimistic scenarios with a small Higgs triplet vacuum expectation value $v_\Delta < 10^{-4}$ GeV, one can look for clean signals of lepton number violation in the decays of doubly charged ($H^{\pm\pm}$) and singly charged ($H^{\pm}$) Higgs bosons to distinguish the Normal Hierarchy (NH), the Inverted Hierarchy (IH) and the Quasi-Degenerate (QD) spectrum for the light neutrino masses. The observation of either $H^+ \to \tau^+ \bar{\nu}$ or $H^+ \to e^+ \bar{\nu}$ will be particularly robust for the spectrum test since they are independent of the unknown Majorana phases. The H^{++} decays moderately depend on a Majorana phase Φ_2 in the NH, but sensitively depend on Φ_1 in the IH. In a less favorable scenario $v_\Delta > 2 \times 10^{-4}$ GeV, when the leptonic channels are suppressed, one needs to observe the decays $H^+ \to W^+ H_1$ and $H^+ \to t\bar{b}$ to confirm the triplet-doublet mixing which in turn implies the existence of the same gauge-invariant interaction between the lepton doublet and the Higgs triplet responsible for the neutrino mass generation. In the most optimistic situation, $v_\Delta \sim 10^{-4}$ GeV, both channels of the lepton pairs and gauge boson pairs may be available simultaneously. The determination of their relative branching fractions would give a measurement for the value of v_Δ.

[*]Electronic address: fileviez@physics.wisc.edu

[†]Electronic address: than@hep.wisc.edu

[‡]Electronic address: ghuang@hep.wisc.edu

[§]Electronic address: tli8@wisc.edu

[¶]Electronic address: wangkai@hep.wisc.edu

I. INTRODUCTION

The existence of massive neutrinos [1] is a strong motivation for physics beyond the Standard Model (SM). As pointed out a long time ago by Weinberg [2], there is just one dimension-five operator relevant for neutrino masses in the context of the Standard Model: $(\kappa/\Lambda)\, l_L l_L H H$, where l_L and H are the leptonic and Higgs $SU(2)_L$ doublets. After the electroweak symmetry breaking (EWSB), the Majorana mass of the neutrinos reads as $m_\nu \sim \kappa v_0^2/\Lambda$, where $v_0 \approx 246$ GeV is the SM Higgs vacuum expectation value (vev). The smallness of $m_\nu \lesssim 1$ eV is thus understood by the "seesaw" spirit if $\Lambda \gg v_0$. Assuming that the coupling κ of the dimension-five operator is the order of unity, the observed neutrino masses imply that $\Lambda \lesssim 10^{14-15}$ GeV. The crucial issue is to understand the origin of this operator in a given extension of the SM in order to identify the dimensionless coupling κ and the mass scale Λ at which the new physics enters. This dimension five operator thus guides us to look for extensions of Standard Model in which the neutrino masses are generated in a UV complete formalism.

There are four simple renormalizable extensions of the Standard Model with minimal addition to generate neutrino Majorana masses conceivable to agree with the experimental observations:

- *Type I seesaw mechanism* [3]: One can add at least two fermionic singlets N_i and the neutrino masses are $m_\nu \sim y_D^2 v_0^2/M_N$, where y_D is the Yukawa coupling and M_N is the right-handed neutrino mass, which sets the new physics scale Λ. If $y_D \simeq 1$ and $M_N \approx 10^{14-15}$ GeV, one obtains the natural value for the neutrino masses $m_\nu \approx 1$ eV.

- *Type II seesaw mechanism* [4]: The Higgs sector of the Standard Model is extended by adding an $SU(2)_L$ Higgs triplet Δ. The neutrino masses are $m_\nu \approx Y_\nu v_\Delta$, where v_Δ is the vacuum expectation value (vev) of the neutral component of the triplet and Y_ν is the Yukawa coupling. With a doublet and triplet mixing via a dimensional parameter μ, the EWSB leads to a relation $v_\Delta \sim \mu v_0^2/M_\Delta^2$, where M_Δ is the mass of the triplet. In this case the scale Λ is replaced by M_Δ^2/μ, and a natural setting would be for $Y_\nu \approx 1$ and $\mu \sim M_\Delta \approx 10^{14-15}$ GeV.

- *Type III seesaw mechanism* [5]: Adding at least two extra matter fields in the adjoint representation of $SU(2)_L$ and with zero hypercharge, one can generate neutrino masses, $m_\nu \sim y^2 v_0^2/M$. Therefore, the high scale Λ is replaced by the mass of the extra fermions in the adjoint representation.

- *Hybrid seesaw mechanism* [6]: One SM fermionic singlet N and one fermion in the adjoint representation of $SU(2)_L$ are added. This is a combination of Type I and Type III but with the same minimal fermionic content. This mechanism has a very simple and unique realization in the context of grand unified theories [6].

In the case of Left-Right symmetric models [7] both Type I and Type II seesaw are present. Alternatively, neutrino masses can be generated by radiative corrections [8].

To test the above seesaw mechanisms one needs to search for the effects of lepton number violation in their unique way. In particular, direct observations of the new heavy states responsible for the seesaw mechanisms would be more conclusive. While the seesaw spirit resides in the existence of a much higher scale $\Lambda \gg v_0$, rendering the new states experimentally inaccessible in the foreseeable future, this may not be necessary the case. For recent studies where the seesaw mechanism could happen at a very low scale see [9]. A light $SU(2)_L$ triplet field responsible for Type II seesaw can be present in the context of a minimal grand unified theory [10]. Low scale Type III seesaw was also studied in [11].

The Large Hadron Collider (LHC) at CERN will soon take us to a new frontier with unprecedented high energy and luminosity. Major discoveries of exciting new physics at the Terascale are highly anticipated. It is thus pressing to investigate the physics potential of the LHC in connection with the new physics for the neutrino mass generation. Searching for heavy Majorana neutrinos at hadron colliders have been considered by many authors [12]. The interests for the LHC have been lately renewed [13, 14, 15]. However, it is believed that any signal of N would indicate a more subtle mechanism beyond the simple Type I seesaw due to the otherwise naturally small mixing $V_{N\ell}^2 \sim m_\nu / M_N$ between N and the SM leptons.

In this paper, we investigate the possibility to test the Type II seesaw mechanism at the LHC. Several earlier studies for certain aspects of the Type II seesaw model at the LHC exist [16, 17, 18, 19, 20, 21, 22]. We systematically explore the parameter space in the model. Guided by the neutrino oscillation experiments, we first establish the preferred parameter regions by reproducing the light neutrino mass and mixing patterns. We then go on to predict the corresponding signatures at the LHC. We find that in the optimistic scenarios, by identifying the flavor structure of the lepton number violating decays of the charged Higgs bosons, one can establish the neutrino mass pattern of the Normal Hierarchy, Inverted Hierarchy or Quasi-Degenerate. We emphasize the crucial role of the singly charged Higgs boson decays. The associated pair production of $H^{\pm\pm}H^{\mp}$ is essential to test the triplet nature of the Higgs field. The observation of either $H^+ \to \tau^+\bar{\nu}$ or $H^+ \to e^+\bar{\nu}$ will be particularly robust for the test since they are independent of the unknown Majorana phases. Combining with the doubly charged Higgs decay, for instance $H^{++} \to e^+\mu^+, e^+\tau^+, \mu^+\tau^+$, one will even be able to probe the Majorana phases. We investigate in great detail all the issues mentioned above, showing all the possibilities to test this appealing mechanism for the neutrino masses at the Large Hadron Collider. A summary of our main results appeared in an early publication [23].

The outline of the paper is as follows: In Section II we present the Type II seesaw mechanism and discuss its main predictions. In Section III the constraints on the physical Higgs couplings coming from neutrino oscillation experiments are investigated. The general features of the Higgs decays are discussed in

Section IV. In Section V we study the predictions for the Higgs decays in this theory. Taking into account the effect of neutrino masses and mixing we show the different predictions for the branching fractions of all lepton number violating decays $H^{++} \rightarrow e_i^+ e_j^+$ and $H^+ \rightarrow e_i^+ \bar{\nu}$, where $e_i = e, \mu, \tau$. We discuss the possibility to identify the spectrum for neutrino masses if all the lepton violating decays are measured at the LHC or at future colliders. The possibility to get the information about the Majorana phases from Higgs decays is discussed. The most important production mechanisms at the LHC are discussed in Section VI. In Section VII, we discuss the necessary steps for testing the Type II seesaw at the LHC, and we draw our conclusions.

II.   THE TYPE II SEESAW MECHANISM FOR NEUTRINO MASSES

The Type II seesaw mechanism [4] is one of the most appealing scenarios for the generation of neutrino masses. In this section we discuss in detail this mechanism and its main predictions. In order to realize the so-called Type II seesaw mechanism for neutrino masses one has to extend the Higgs sector of the Standard Model. In this case the Higgs sector of the theory is composed of the SM Higgs $H \sim (1, 2, 1/2)$ and an $SU(2)_L$ scalar triplet $\Delta \sim (1, 3, 1)$. The matrix representation of the triplet reads as

$$\Delta = \begin{pmatrix} \delta^+/\sqrt{2} & \delta^{++} \\ \delta^0 & -\delta^+/\sqrt{2} \end{pmatrix}. \tag{1}$$

The kinetic terms and the relevant interactions in this theory are given by

$$\mathcal{L}_{\text{TypeII}} = (D_\mu H)^\dagger (D^\mu H) + \text{Tr}(D_\mu \Delta)^\dagger (D^\mu \Delta) + \mathcal{L}_Y - V(H, \Delta), \tag{2}$$

where the needed interaction to generate neutrino masses reads as

$$\mathcal{L}_Y = -Y_\nu \, l_L^T \, C \, i\sigma_2 \, \Delta \, l_L + \text{h.c.}, \tag{3}$$

and the scalar interactions are given by

$$V(H, \Delta) = -m_H^2 \, H^\dagger H + \frac{\lambda}{4}(H^\dagger H)^2 + M_\Delta^2 \, Tr\Delta^\dagger\Delta + \left(\mu \, H^T \, i\sigma_2 \, \Delta^\dagger H + h.c.\right) +$$
$$+ \, \lambda_1 \, (H^\dagger H) Tr\Delta^\dagger\Delta + \lambda_2 \left(Tr\Delta^\dagger\Delta\right)^2 + \lambda_3 \, Tr\left(\Delta^\dagger\Delta\right)^2 + \lambda_4 \, H^\dagger\Delta\Delta^\dagger H. \tag{4}$$

In the above equations the Yukawa coupling Y_ν is a 3×3 symmetric complex matrix. $l_L^T = (\nu_L^T, \, e_L^T)$, C is the charge conjugation operator, and σ_2 is the Pauli matrix. Since we are mainly interested in a heavy Higgs triplet, typically $M_\Delta^2 > v_0^2/2$, we will neglect the contributions coming from the terms proportional to λ_1, λ_2, λ_3 and λ_4. The detailed structure and interactions of this Higgs sector will be presented in Appendix A.

Let us discuss some important features of this model for neutrino masses:

- Imposing the conditions of global minimum one finds that

$$-m_H^2 + \frac{\lambda}{4}v_0^2 - \sqrt{2}\,\mu\,v_\Delta = 0, \qquad \text{and} \qquad v_\Delta = \frac{\mu\,v_0^2}{\sqrt{2}\,M_\Delta^2}, \qquad (5)$$

where v_0 and v_Δ are the vacuum expectation values of the Higgs doublet and triplet, respectively, with $v_0^2 + v_\Delta^2 \approx (246\,\text{GeV})^2$. Due to the simultaneous presence of the Yukawa coupling Y_ν in Eq. (3), and the term proportional to the μ parameter in Eq. (4), the lepton number is explicitly broken in this theory. Therefore, one expects that the neutrino Majorana mass term has to be proportional to $Y_\nu \times \mu$.

- Once the neutral component in Δ gets the vev, v_Δ as in Eq. (5), the neutrinos acquire a Majorana mass given by the following expression:

$$M_\nu = \sqrt{2}\,Y_\nu\,v_\Delta = Y_\nu\,\frac{\mu\,v_0^2}{M_\Delta^2}, \qquad (6)$$

which is the key relation for the Type II seesaw scenario.

- After the electroweak symmetry breaking, there are seven physical massive Higgs bosons left in the spectrum:

$$H_1 = \cos\theta_0\,h^0 + \sin\theta_0\,\Delta^0, \quad H_2 = -\sin\theta_0\,h^0 + \cos\theta_0\Delta^0, \qquad \text{with } \theta_0 \approx \frac{2v_\Delta}{v_0}, \quad (7)$$

$$A = -\sin\alpha\,\xi^0 + \cos\alpha\,\eta^0, \qquad \text{with} \qquad \alpha \approx \frac{2v_\Delta}{v_0}, \qquad (8)$$

$$H^\pm = -\sin\theta_\pm\,\phi^\pm + \cos\theta_\pm\,\delta^\pm, \qquad \text{with} \qquad \theta_+ \approx \frac{\sqrt{2}v_\Delta}{v_0}, \qquad (9)$$

$$\text{and} \qquad H^{\pm\pm} = \delta^{\pm\pm}, \qquad \text{with mass} \qquad M_{\delta++} = M_\Delta, \qquad (10)$$

where H_1 is SM-like (doublet) while the rest of the Higgs states are all Δ-like (triplet), and

$$M_{H_2} \simeq M_A \simeq M_{H^\pm} \simeq M_{H^{++}} = M_\Delta.$$

- Working in the physical basis for the fermions we find that the Yukawa interactions can be written as

$$\nu_L^T\,C\,\Gamma_+\,H^+\,e_L, \qquad \text{and} \qquad e_L^T\,C\,\Gamma_{++}\,H^{++}\,e_L, \qquad (11)$$

where

$$\Gamma_+ = \cos\theta_+\,\frac{m_\nu^{diag}}{v_\Delta}\,V_{PMNS}^\dagger, \qquad \text{and} \qquad \Gamma_{++} = V_{PMNS}^*\,\frac{m_\nu^{diag}}{\sqrt{2}\,v_\Delta}\,V_{PMNS}^\dagger = Y_\nu. \quad (12)$$

The values of the physical couplings Γ_+ and Γ_{++} are thus governed by the spectrum and mixing angles for the active neutrinos. Therefore, one can expect that the lepton-number violating decays of the Higgs bosons, $H^{++} \to e_i^+ e_j^+$ and $H^+ \to e_i^+ \bar\nu$ ($e_i = e, \mu, \tau$) will be characteristically different in each spectrum for neutrino masses.

- Higgs-Gauge Interactions: The doubly charged Higgs has only one coupling to gauge bosons, $H^{\pm\pm}W^{\mp}W^{\mp}$, which is proportional to the vev of the triplet field v_Δ. In the case of the singly charged Higgs there are two relevant couplings for the decays into gauge bosons, $H^{\pm}W^{\mp}H_1$ and $H^{\pm}W^{\mp}Z$. As for the heavy neutral Higgs H_2 one finds that its coupling to W's is further suppressed. The only relevant couplings for the decays are H_2ZZ and $H_2H_1H_1$, see Appendix A for details.

These are the main properties and predictions of this simple extension of the Standard Model where the neutrino masses are generated through the Type II seesaw mechanism.

III.   CONSTRAINTS ON THE PHYSICAL PARAMETERS

In this section we discuss the constraints coming from neutrino experiments, rare decays and collider experiments on the physical parameters in this theory for neutrino masses.

A.   Constraints From Neutrino Oscillation Experiments

The relevant physical Yukawa couplings of the singly and doubly charged Higgs bosons for the leptonic decays are given by Eq. (12). In order to understand the constraints coming from neutrino physics let us discuss the relation between the neutrino masses and mixing. The leptonic mixing matrix is given by

$$V_{PMNS} = \begin{pmatrix} c_{12}c_{13} & c_{13}s_{12} & e^{-i\delta}s_{13} \\ -c_{12}s_{13}s_{23}e^{i\delta} - c_{23}s_{12} & c_{12}c_{23} - e^{i\delta}s_{12}s_{13}s_{23} & c_{13}s_{23} \\ s_{12}s_{23} - e^{i\delta}c_{12}c_{23}s_{13} & -c_{23}s_{12}s_{13}e^{i\delta} - c_{12}s_{23} & c_{13}c_{23} \end{pmatrix} \times \mathrm{diag}(e^{i\Phi_1/2}, 1, e^{i\Phi_2/2}) \quad (13)$$

where $s_{ij} = \sin\theta_{ij}$, $c_{ij} = \cos\theta_{ij}$, $0 \leq \theta_{ij} \leq \pi/2$ and $0 \leq \delta \leq 2\pi$. The phase δ is the Dirac CP-violating phase, while Φ_i are the Majorana phases. The experimental constraints on the neutrino masses and mixing parameters, at 2σ level [24], are

$$7.3 \times 10^{-5} \, \mathrm{eV}^2 \quad < \quad \Delta m_{21}^2 \quad < \quad 8.1 \times 10^{-5} \, \mathrm{eV}^2, \tag{14}$$

$$2.1 \times 10^{-3} \, \mathrm{eV}^2 \quad < \quad |\Delta m_{31}^2| \quad < \quad 2.7 \times 10^{-3} \, \mathrm{eV}^2, \tag{15}$$

$$0.28 \quad < \quad \sin^2\theta_{12} \quad < \quad 0.37, \tag{16}$$

$$0.38 \quad < \quad \sin^2\theta_{23} \quad < \quad 0.63, \tag{17}$$

$$\sin^2\theta_{13} \quad < \quad 0.033, \tag{18}$$

and from cosmological observations

$$\sum_{i=1}^{3} m_i < 1.2 \text{ eV}. \tag{19}$$

For a complete discussion of these constraints see reference [1]. In this section we focus mainly on the case of Normal Hierarchy (NH), $\Delta m_{31}^2 > 0$, and Inverted Hierarchy (IH) spectrum, $\Delta m_{31}^2 < 0$, neglecting the Majorana phases.

Using the above experimental constraints, we first show the allowed values for the neutrino mass matrix M_ν as seen in Figs. 1 and 2, as a function of the lightest neutrino mass. These results directly reflect the patterns of the neutrino mass and mixing: $M_\nu^{11} \ll M_\nu^{22}, M_\nu^{33}$ in the case of NH in Fig. 1(a), and $M_\nu^{11} > M_\nu^{22}, M_\nu^{33}$ in the case of IH in Fig. 1(b). For the off-diagonal elements, M_ν^{23} takes the largest values in each spectrum due to the large atmospheric mixing angle as seen in Fig. 2. Also seen is the "quasi-degenerate" case for $m_1 \approx m_2 \approx m_3 > |\Delta m_{31}|$, where the flavor-diagonal elements are about equal. Since $\Gamma_{++} = M_\nu/\sqrt{2}v_\Delta$, the constraints on the neutrino mass matrix elements directly translate into the physical couplings of H^{++} that govern its decay widths. As for the coupling of the singly charged Higgs boson, we sum over the final state neutrinos since they are experimentally unobservable. Thus the relevant couplings are written as

$$Y_+^i \equiv \sum_{j=1}^{3} |\Gamma_+^{ji}|^2 v_\Delta^2 \quad (i = 1, 2, 3 \text{ for charged leptons } e, \mu, \tau). \tag{20}$$

The allowed values are shown in Fig. 3. Similar to the situations for H^{++}, $Y_+^1 \ll Y_+^2, Y_+^3$ in the NH and $Y_+^1 > Y_+^2, Y_+^3$ in the IH.

B.   Rare Decays

The charged Higgs bosons may mediate tree-level lepton flavor violation processes, leading to some stringent constraints on the model parameters, see reference [25] for a recent comprehensive analysis. In the model under consideration, the most important constraint comes from the process $\mu \to 3e$ via the doubly charged Higgs. The branching fraction is given by

$$\text{BR}(\mu \to 3e) \simeq \frac{\Gamma(\mu \to 3e)}{\Gamma(\mu \to e\,\nu_\mu\,\bar\nu_e)} = \frac{|\Gamma_{++}^{11}\,\Gamma_{++}^{12}|^2}{4\,M_\Delta^4\,G_F^2}. \tag{21}$$

Using the experimental upper bound listed in [26], $\text{BR}(\mu \to 3e) < 10^{-12}$, one finds

$$|\Gamma_{++}^{11}\,\Gamma_{++}^{12}| < 2.4 \times 10^{-5} \times \left(\frac{M_\Delta}{1 \text{ TeV}}\right)^2. \tag{22}$$
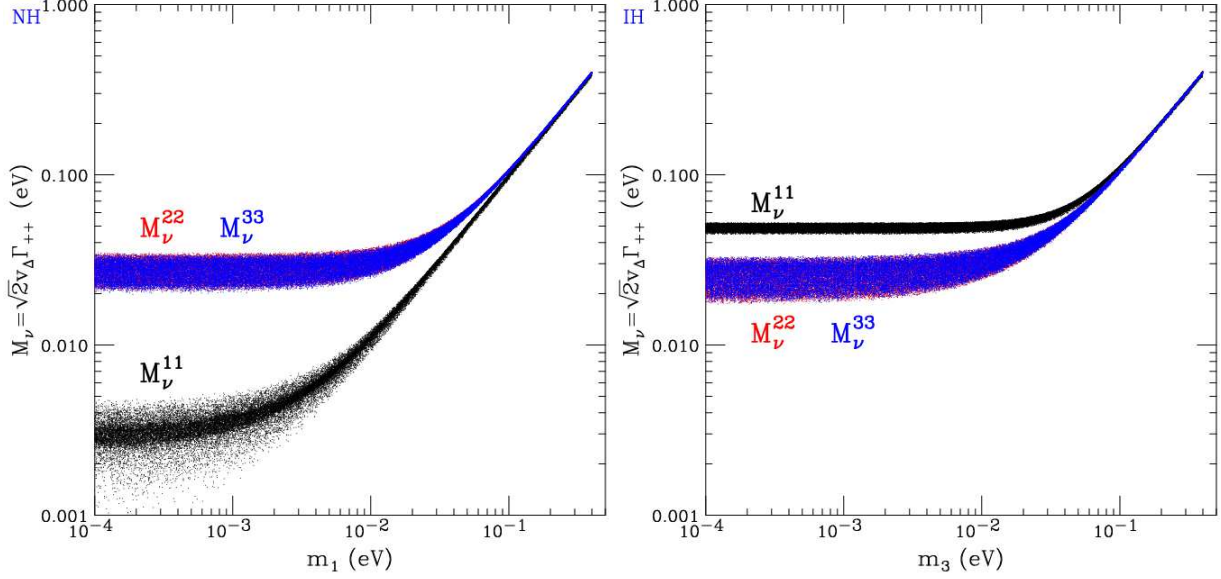
FIG. 1: Constraints on the diagonal elements of the neutrino mass matrix M_ν versus the lowest neutrino mass for (a) NH (left) and (b) IH (right) when $\Phi_1 = 0$ and $\Phi_2 = 0$.
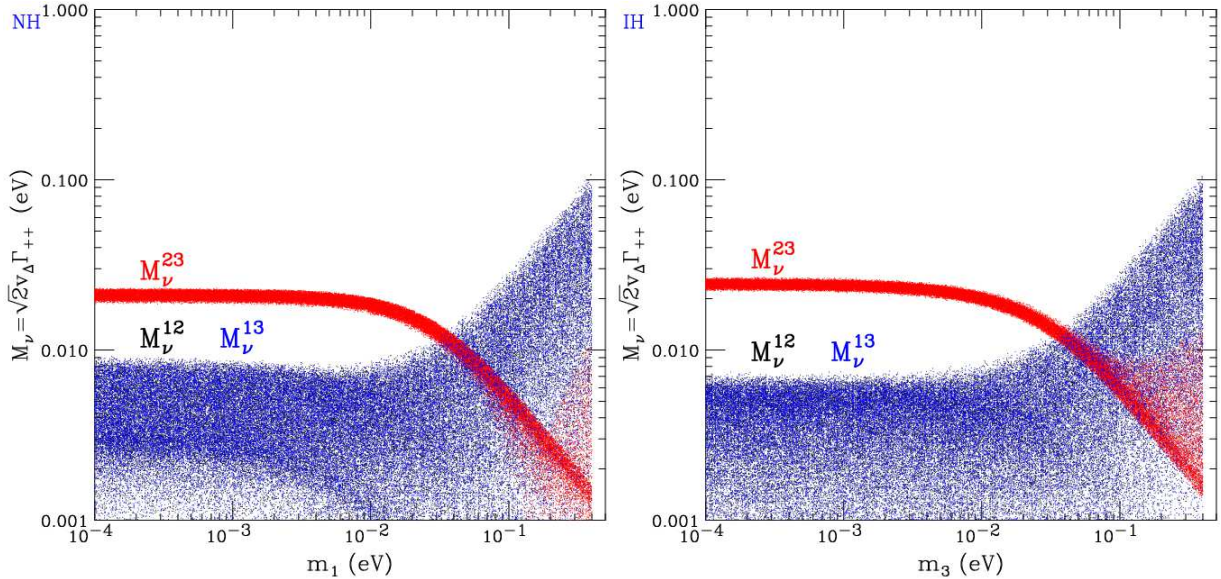

FIG. 2: Constraints on the off-diagonal elements of the neutrino mass matrix M_ν versus the lowest neutrino mass for (a) NH (left) and (b) IH (right) when $\Phi_1 = 0$ and $\Phi_2 = 0$.

This in turn, combining with the relation between the Yukawa couplings and the neutrino mass matrix, gives a lower bound on the vev for a given value of the triplet mass

$$v_\Delta^2 \; > \; 0.2 \times 10^5 \, |M_\nu^{11} M_\nu^{12}| \times \left(\frac{1\,\text{TeV}}{M_\Delta} \right)^2 . \tag{23}$$
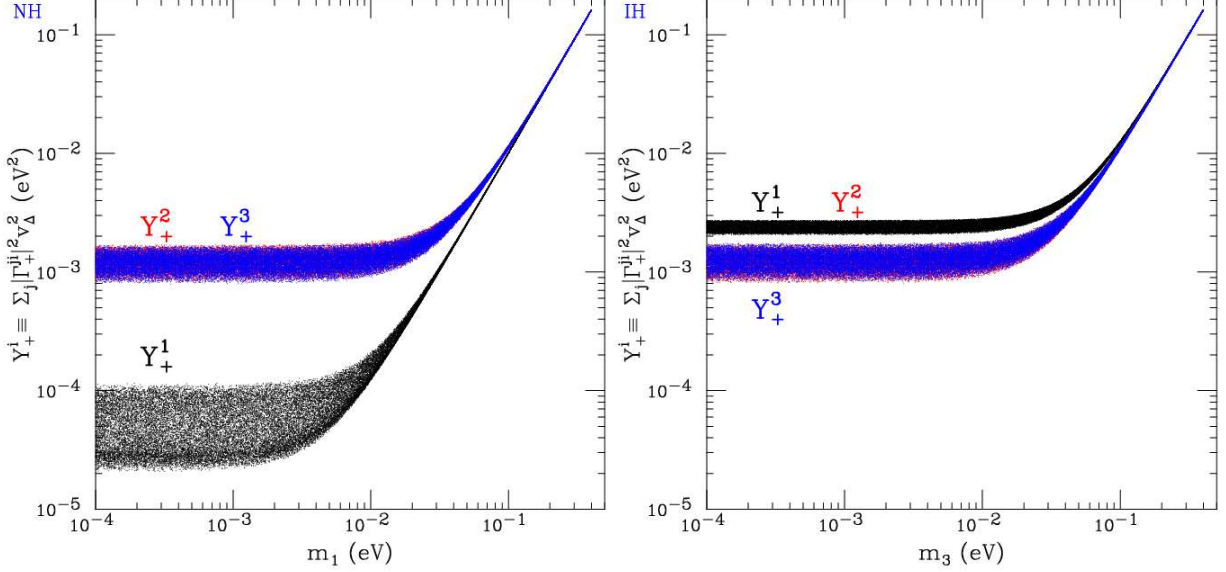
FIG. 3: Constraints on the coupling squared for H^+, $Y_+^i \equiv \sum_j |\Gamma_+^{ji}|^2 v_\Delta^2$, versus the lowest neutrino mass for (a) NH (left) and (b) IH (right).

Even in the conservative case, the IH scenario where $\sqrt{M_\nu^{11} M_\nu^{12}}$ is as large as 0.02 eV, and for $M_\Delta \sim$ 1 TeV, one obtains $v_\Delta \gtrsim 2$ eV, which is not very relevant for our interest.

C. Other Constraints

There are two dimensionful free parameters M_Δ and v_Δ in this theory for neutrino masses. The current constraint on M_Δ comes from the direct search for $H^{\pm\pm}$ at the Tevatron [27]

$$M_\Delta \gtrsim 110 \text{ GeV}. \tag{24}$$

The vev of the triplet,

$$1 \text{ eV} \lesssim v_\Delta \lesssim 1 \text{ GeV}, \tag{25}$$

where the lower bound is based on the naturalness consideration from neutrino masses, and upper bound is from the constraint of the electroweak ρ-parameter [28].

IV. GENERAL FEATURES OF HIGGS DECAYS

In this section we study all decays of the physical Higgs bosons in the theory neglecting the leptonic mixings. In this theory one has seven physical Higgs bosons, the CP-even neutral scalars H_1 (SM-like),
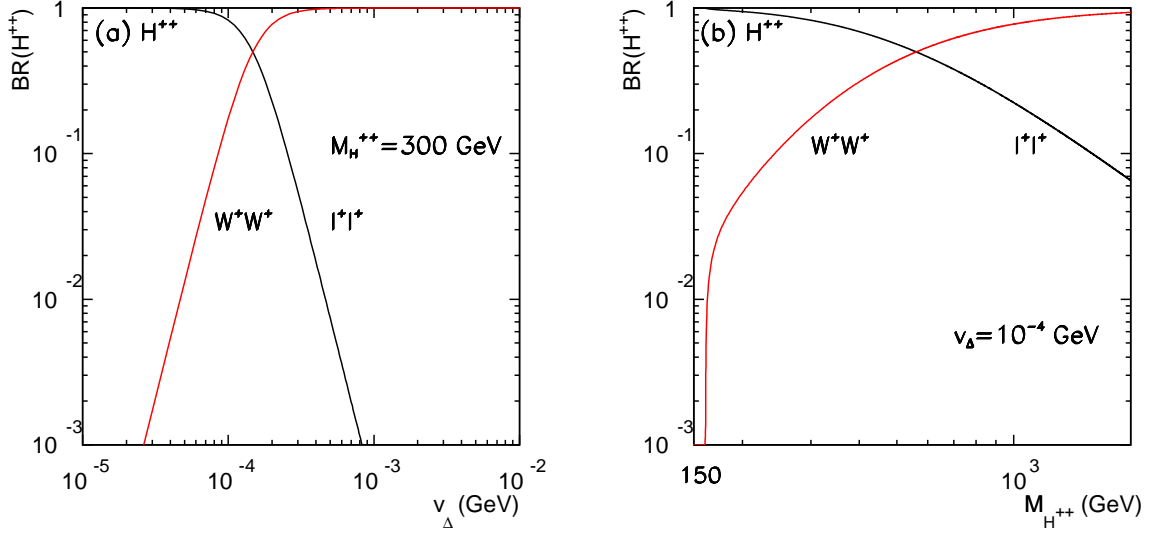
FIG. 4: Branching fractions of the doubly charged Higgs boson decay versus (a) v_Δ for $M_{H^{++}} = 300$ GeV, and (b) $M_{H^{++}}$ for $v_\Delta = 10^{-4}$ GeV.

and H_2 (Δ-like), a CP-odd neutral scalar A, two singly charged Higgs bosons $H^\pm$, and two doubly charged Higgs bosons $H^{\pm\pm}$. Their decay partial widths are given in Appendix B.

A. Doubly Charged Higgs Boson Decays

The possible decays of the doubly charged Higgs bosons, $H^{\pm\pm}$, are the lepton number violating decays $H^{++} \rightarrow e_i^+ e_j^+$, where $e_i = e, \mu, \tau$, and the decays into two W's. The decay rates for the lepton number violating decays are:

$$\Gamma\left(H^{++} \rightarrow e_i^+ e_j^+\right) = \frac{|M_\nu^{ij}|^2}{8\pi(1 + \delta_{ij})v_\Delta^2} M_{H^{++}} \tag{26}$$

where M_ν^{ij} is the neutrino mass matrix and δ_{ij} is the Kronecher's delta. In the case of the decays into W's the decay rates are given by

$$\Gamma\left(H^{++} \rightarrow W_T^+ W_T^+\right) = \frac{2M_W^4 v_\Delta^2}{\pi v_0^4 M_{H^{++}}} \left(1 - \frac{4M_W^2}{M_{H^{++}}^2}\right)^{1/2} \tag{27}$$

and

$$\Gamma\left(H^{++} \rightarrow W_L^+ W_L^+\right) = \frac{v_\Delta^2 M_{H^{++}}^3}{4\pi v_0^4} \left(1 - \frac{4M_W^2}{M_{H^{++}}^2}\right)^{1/2} \left(1 - \frac{2M_W^2}{M_{H^{++}}^2}\right)^2 \tag{28}$$

where W_L and W_T stand for the longitudinal and transverse polarizations of the W gauge boson, respectively. The decays into leptons are proportional to the Yukawa coupling for neutrinos while the decays into
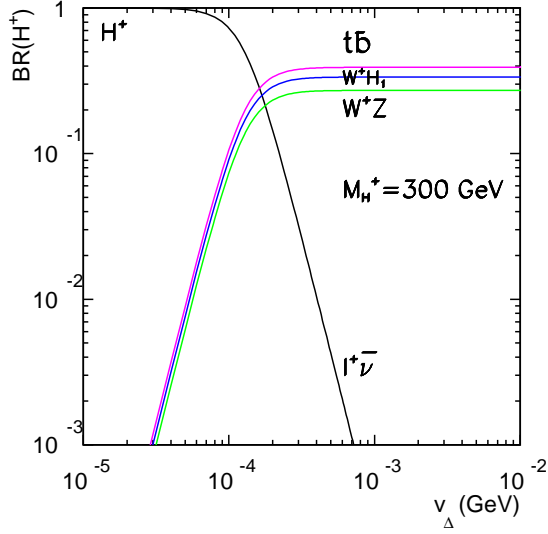
FIG. 5: Branching fractions of the singly charged Higgs boson decay versus v_Δ for $M_{H^+} = 300$ GeV (In our study we use $M_{H_1} = 120$ GeV.).

two W's are proportional to the vev. The relative decay branchings can be estimated by

$$\frac{\Gamma(H^{++} \to e_i^+ e_j^+)}{\Gamma(H^{++} \to W^+ W^+)} \approx \frac{|\Gamma_{++}|^2 M_{H^{++}}}{M_{H^{++}}^3 v_\Delta^2 / v_0^4} \approx \left(\frac{m_\nu}{M_{H^{++}}}\right)^2 \left(\frac{v_0}{v_\Delta}\right)^4. \tag{29}$$

Taking $m_\nu/M_{H^{++}} \sim 1$ eV/1 TeV, one finds that these two decay modes are comparable when $v_\Delta \approx 10^{-4}$ GeV. The branching fractions for the decays of the doubly charged Higgs, BR(H^{++}), are shown in Fig. 4, assuming that the Yukawa matrix Y_ν (or Γ_{++}) is diagonal, for simple illustration. In Fig. 4(a) we plot the branching fractions versus v_Δ for $M_{H^{++}} = 300$ GeV; while in Fig. 4(b) we show BR(H^{++}) versus the doubly charged Higgs mass for $v_\Delta = 10^{-4}$ GeV. As seen from Eq. (29) and the figures, an important feature is that when $v_\Delta < 10^{-4}$ GeV the most important decays are those with a pair of like-sign charged leptons, while for $v_\Delta > 10^{-4}$ GeV the most relevant decays are into two W's.

B. Singly Charged Higgs Boson Decays

In the case of the singly charged Higgs boson, one has the decays $H^+ \to e_i^+ \bar\nu$ proportional to the Yukawa coupling of neutrinos, $H^+ \to W^+ H_1$, $W^+ Z$, and $H^+ \to t\bar b$ proportional to the v_Δ. As in the case of the doubly charged Higgs all decays are connected by the relation $M_\nu = \sqrt{2}\, Y_\nu\, v_\Delta$. In Fig. 5 one can see the relevant decay channels for $M_{H^+} = 300$ GeV versus v_Δ. The most important channels for large values of vev are $H^+ \to t\bar b$, $H^+ \to W^+ H_1$ and $H^+ \to W^+ Z$, while $H^+ \to e_i^+ \bar\nu$ is the dominant channel for small v_Δ when the Higgs mass is below TeV. Here and henceforth, we take $M_{H_1} = 120$ GeV.
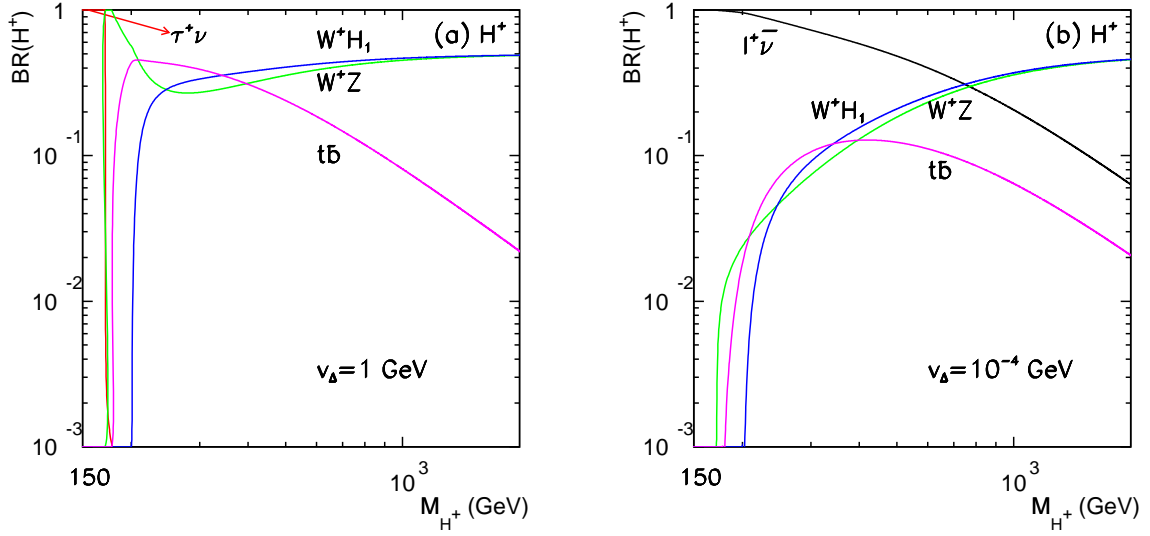
FIG. 6: Branching fractions of the singly charged Higgs boson decay versus its mass for (a) $v_\Delta = 1$ GeV and (b) $v_\Delta = 10^{-4}$ GeV, respectively.

Furthermore,

$$\frac{\Gamma(H^+ \to t\bar{b})}{\Gamma(H^+ \to W^+Z)} \approx \frac{3(v_\Delta m_t/v_0^2)^2 M_\Delta}{M_\Delta^3 v_\Delta^2/2v_0^4} = 6\left(\frac{m_t}{M_\Delta}\right)^2.$$

Thus the decays $H^+ \to W^+Z$, W^+H_1 dominate over $t\bar{b}$ for $M_\Delta > 400$ GeV.

In Fig. 6(a) and Fig. 6(b) we plot the branching fractions of the singly charged Higgs boson versus its mass for $v_\Delta = 1$ GeV and $v_\Delta = 10^{-4}$ GeV, respectively. In Fig. 6(a), below the WZ threshold, it is irrelevant to our collider search so we neglect the offshell W^*/Z^* decay channels then $H^+ \to \tau^+\nu$ is dominant.

C.   CP-Even Heavy Higgs Boson Decays

The decays of the heavy neutral CP-even neutral scalar H_2 (Δ-like) are shown in Figs. 7 and 8. The most relevant decays are $H_2 \to H_1H_1$, ZZ, $b\bar{b}$, $t\bar{t}$ proportional to v_Δ, and the decays into a pair of neutrinos proportional to the Yukawa couplings. As for all physical Higgs bosons in the theory all decays are connected by the neutrino mass relation in Eq. (6). As we can appreciate from the Figs. 7 and 8 when the v_Δ is large $H_2 \to H_1H_1$ and $H_2 \to ZZ$ are the most relevant channels. In this model the channel $H_2 \to W^+W^-$ is highly suppressed being zero at leading order (see Appendix B for details). As one expects the decays into neutrinos and antineutrinos become important below $M_\Delta \sim$ TeV and for small v_Δ.
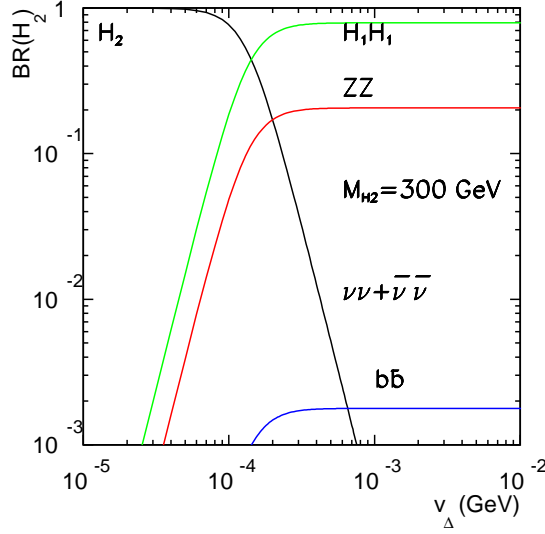
FIG. 7: Branching fractions of the heavy CP-even Higgs boson decay versus v_Δ for $M_{H_2} = 300$ GeV.
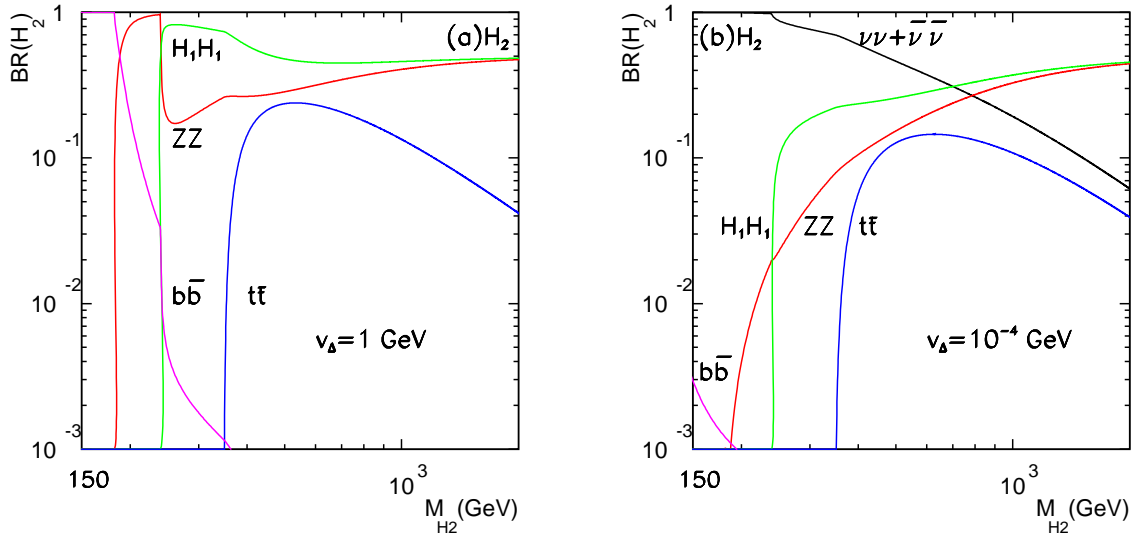

FIG. 8: Branching fractions of the heavy CP-even Higgs boson decay versus its mass for (a) $v_\Delta = 1$ GeV and (b) $v_\Delta = 10^{-4}$ GeV, respectively.

D. CP-Odd Heavy Higgs Boson Decays

The relevant decays of the CP-odd scalar field A are $A \to t\bar{t}, H_1 Z$ and the decays into neutrinos and antineutrinos. The branching fractions of A for $M_A = 300$ GeV and different values of v_Δ are shown in Fig. 9. In Fig. 10 we plot the different decays of A for $v_\Delta = 1$ GeV and $v_\Delta = 10^{-4}$ GeV, respectively.
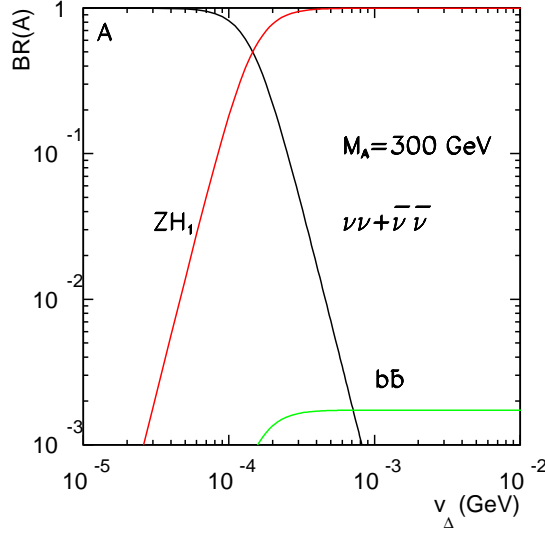
FIG. 9: Branching fractions of the heavy CP-odd Higgs boson decay versus v_Δ for $M_A = 300$ GeV.
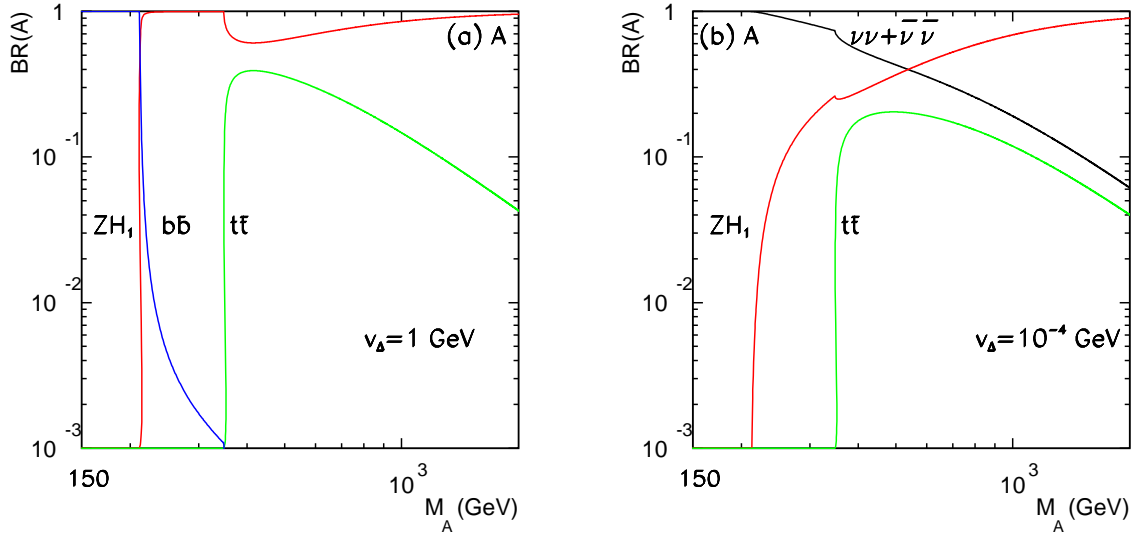
FIG. 10: Branching fractions of the heavy CP-odd Higgs boson decay versus its mass for (a) $v_\Delta = 1$ GeV and (b) $v_\Delta = 10^{-4}$ GeV, respectively.

As in the previous cases the decays into neutrinos and antineutrinos are the most relevant for large Yukawa couplings and in the low mass region. Notice that the decay $A \to ZH_1$ is the dominant one for large values of v_Δ. From this discussion one can conclude that the lepton number violating decays of the different physical Higgs bosons, $H_2, A, H^\pm$, and $H^{\pm\pm}$, in the theory dominate for small values of the triplet vacuum expectation value.
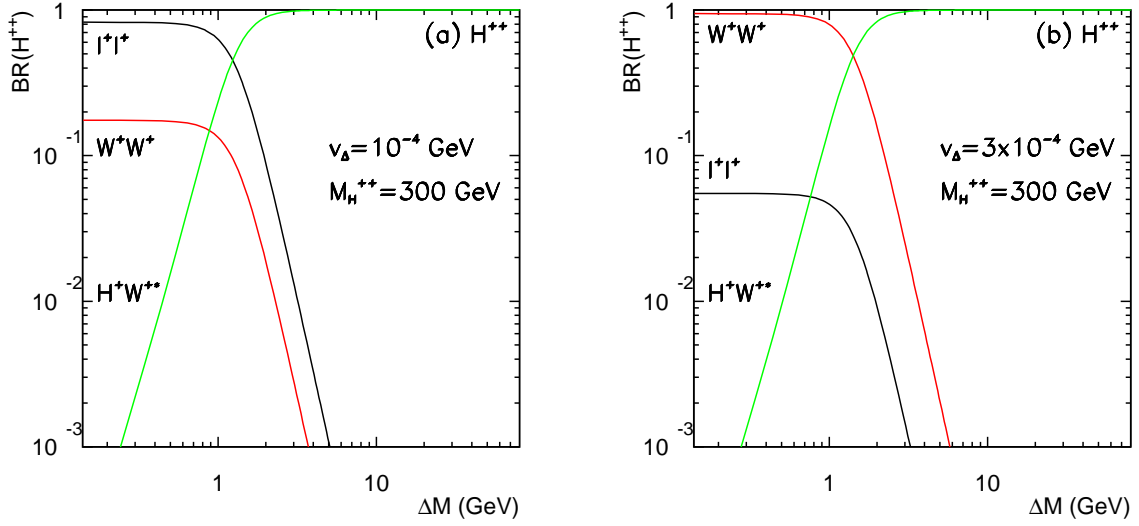
FIG. 11: Branching fractions of the doubly charged Higgs boson decay versus the mass splitting $\Delta M \equiv M_{H^{++}} - M_{H^+}$ for (a) $v_\Delta = 10^{-4}$ GeV and (b) $v_\Delta = 3 \times 10^{-4}$ GeV, respectively.

E.   Mass Splitting And Heavy-to-Heavy Transition via Gauge Interactions

In our discussions thus far, we have assumed the mass degeneracy for the triplet-like Higgs bosons. According to Eq. (4), a tree level mass splitting can be generated and the squared mass difference of the doubly and singly charged Higgs bosons is given by $\lambda_4 v_0^2/4$. Even if there is no tree-level mass difference under our assumption $\lambda_i = 0$, the SM gauge bosons generate the splitting of the masses via radiative corrections at one-loop [29], leading to $\Delta M \equiv M_{H^{++}} - M_{H^+} \approx 540$ MeV.

A small mass difference will make no appreciable effects for the Higgs production. However, the transitions between two heavy triplet Higgs bosons via the SM gauge interactions, such as

$$H^{++} \to H^+ W^{+*}, \quad H^+ \to H^0 W^{+*} \tag{30}$$

may be sizable if kinematically accessible. Their partial decay widths are given in Appendix B. In Fig. 11 we calculate the decay branching fractions of the doubly charged Higgs versus the mass splitting for $v_\Delta = 10^{-4}$ GeV and $v_\Delta = 3 \times 10^{-4}$ GeV, taking into account $H^{++} \to H^+ M^+$ ($M^+ = \pi^+, K^+...$), $H^+ e_i^+ \nu$ ($e_i = e, \mu, \tau$) and $H^+ q\bar{q}'$. We find that the heavy-to-heavy transition can be dominant for $\Delta M > 1$ GeV. With our current assumption, $\Delta M = 540$ MeV [29], the decay branching fractions are shown in Fig. 12 versus the triplet vev. We see that the decay mode $H^{++} \to H^+(W^+)^*$ is subleading and will be neglected in the rest of our discussions.
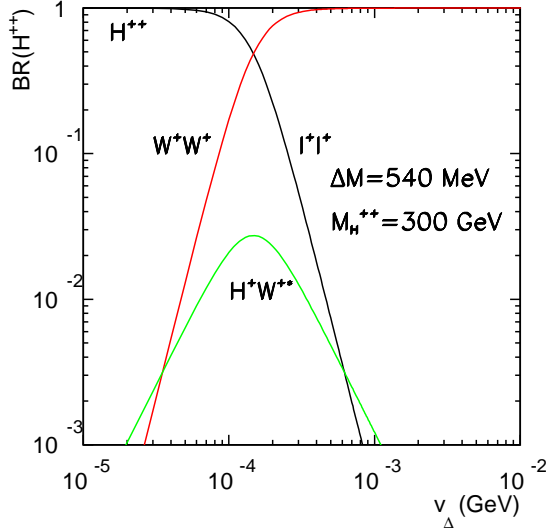
FIG. 12: Branching fractions of the doubly charged Higgs boson decay versus v_Δ for $\Delta M = 540$ MeV.

V.   HIGGS BOSON DECAYS IN CONNECTION TO NEUTRINO PROPERTIES

In this section we study the properties of the lepton number violating Higgs decays taking into account the experimental constraints on the neutrino masses and mixing.

A. $H^{++} \rightarrow e_i^+ e_j^+$

In the previous section we have discussed the decays of the doubly charged Higgs showing that below $v_\Delta \approx 10^{-4}$ GeV, the decays of doubly charged Higgs H^{++} are dominated by the leptonic channels. For simplicity, we first ignore the effects of the Majorana phases $\Phi_1 = \Phi_2 = 0$. In Figs. 13 and 14, we show the dramatic impact of the neutrino masses and mixing on the branching ratios for the final states of the same and different flavors, respectively. In the case of the decays with two identical (anti)leptons as in Fig. 13, the branching fraction can differ by two orders of magnitude in the case of a normal hierarchy with $\mathrm{BR}(H^{++} \rightarrow \tau^+\tau^+)$, $\mathrm{BR}(H^{++} \rightarrow \mu^+\mu^+) \gg \mathrm{BR}(H^{++} \rightarrow e^+e^+)$, and about one order of magnitude in the inverted spectrum with $\mathrm{BR}(H^{++} \rightarrow e^+e^+) > \mathrm{BR}(H^{++} \rightarrow \mu^+\mu^+)$, $\mathrm{BR}(H^{++} \rightarrow \tau^+\tau^+)$. The impact is also dramatic for both spectra in the case of the decays with different leptons in the final state with $\mathrm{BR}(H^{++} \rightarrow \mu^+\tau^+) \gg \mathrm{BR}(H^{++} \rightarrow e^+\mu^+)$, $\mathrm{BR}(H^{++} \rightarrow e^+\tau^+)$, as in Fig. 14. These features directly reflect the neutrino mass and mixing patterns. As one expects that all these channels are quite similar when the neutrino spectrum is quasi-degenerate, $m_1 \approx m_2 \approx m_3 \geq 0.1$ eV. The rather large regions of the scatter plots reflect the imprecise values for neutrino masses and leptonic mixings. In the future [30], once those
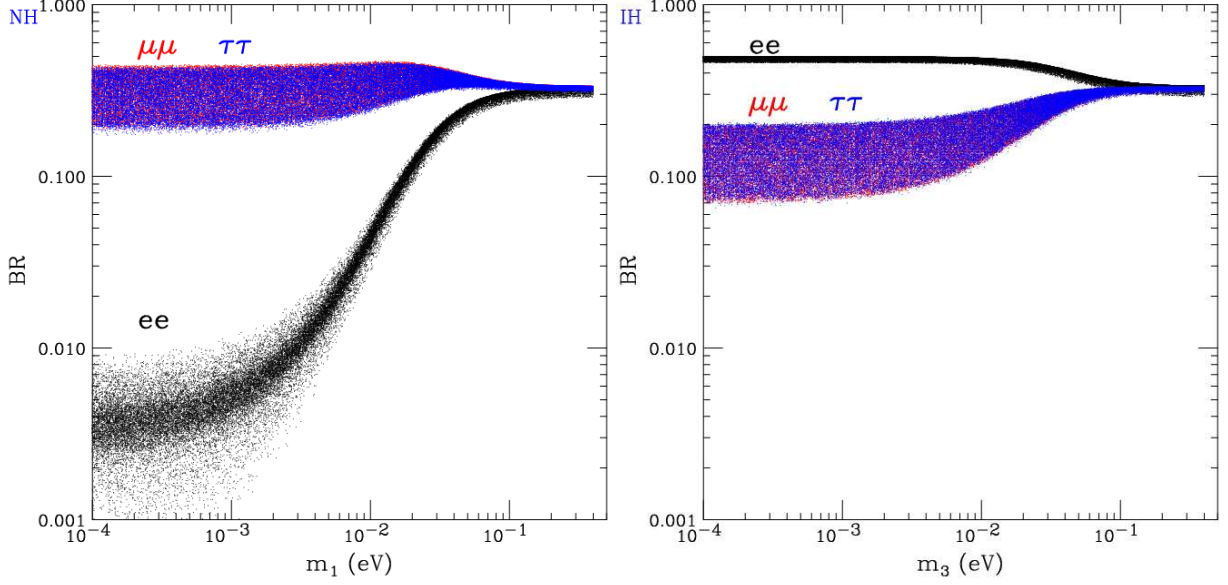
FIG. 13: Scatter plots for the H^{++} decay branching fractions to the flavor-diagonal like-sign dileptons versus the lowest neutrino mass for NH (left) and IH (right) with $\Phi_1 = \Phi_2 = 0$.
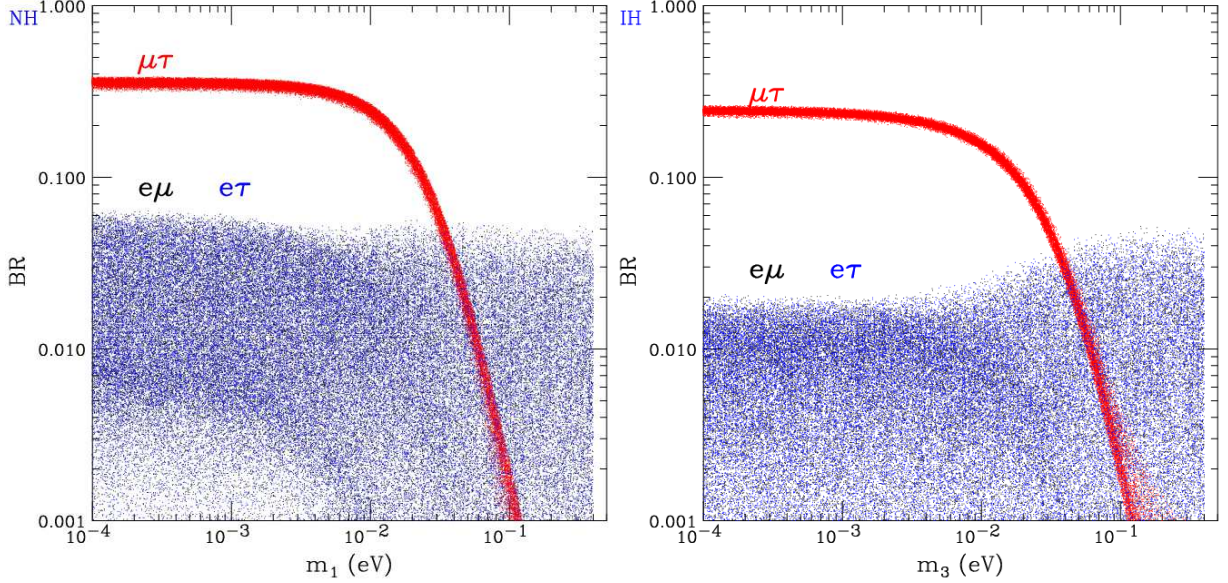

FIG. 14: Same as Fig. 13, but for H^{++} decay to the flavor-off-diagonal like-sign dileptons.

values will be known to a better precision one can improve our predictions for the lepton number violating Higgs decays.

The total decay width of H^{++} depends on the neutrino and Higgs triplet parameters. In terms of v_Δ, the minimal width or the maximal decay length occur near the cross-over between WW-dominant and $\ell\ell$-dominant regions near 10^{-4} GeV. As seen in Fig. 15, the proper decay length can be as large as $c\tau \gtrsim 10\,\mu m$.
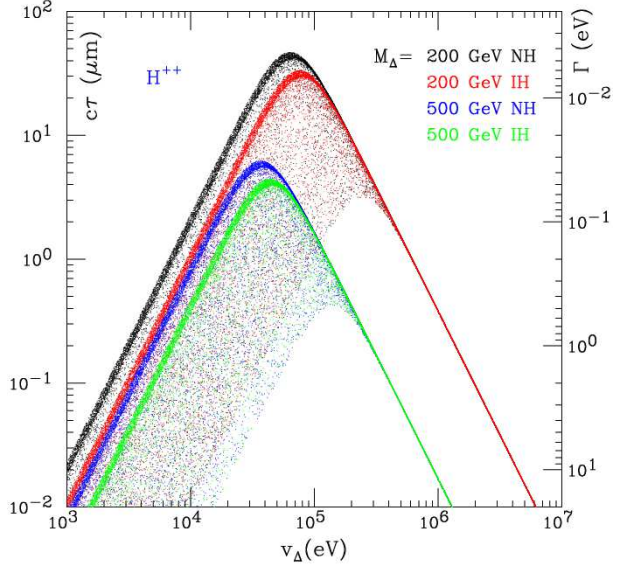
FIG. 15: Decay length and total width of the doubly charged Higgs boson H^{++} with $\Phi_1 = \Phi_2 = 0$.

Although not considered as a long-lived charged particle, the H^{++} decay could lead to a visible displaced vertex in the detector at the LHC.

B. $H^+ \rightarrow e_i^+ \bar{\nu}$

The predictions for the decays of singly charged Higgs boson taking into account the experimental constraints on neutrino mass and mixing parameters are shown in Fig. 16, again ignoring the effects of the Majorana phases $\Phi_1 = \Phi_2 = 0$. The general features are similar to those of H^{++} decays. As one can see in the case of NH the BR$(H^+ \rightarrow \tau^+ \bar{\nu})$ and BR$(H^+ \rightarrow \mu^+ \bar{\nu})$ are dominant, while in the case of IH, the BR$(H^+ \rightarrow e^+ \bar{\nu})$ is the leading one. The maximal decay lengths of the singly charged Higgs is about twice that of the doubly charged Higgs, as shown in Fig. 17.

We now summarize the properties of the lepton-number violating Higgs decays, that are intimately related to the patterns of the neutrino mass and mixing, in Table I, where we have neglected the effects of the Majorana phases.

C.   Impact of Majorana Phases in Higgs Boson Decays

Recently, the effects of Majorana phases on the Higgs decays have been investigated by several groups [19, 20, 21]. Wherever overlap exists, our results are in agreement with theirs. In fact, the effects can be made quite transparent under some simple approximations.
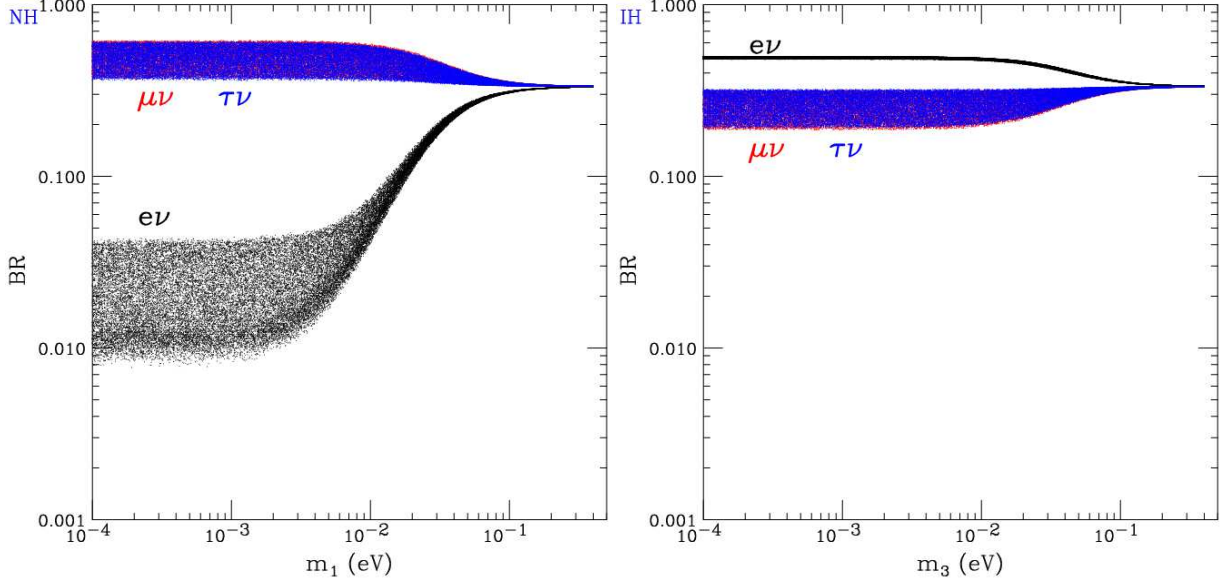
FIG. 16: Scatter plots for the H^+ decay branching fractions to leptons versus the lowest neutrino mass for NH (left) and IH (right) with $\Phi_1 = \Phi_2 = 0$.
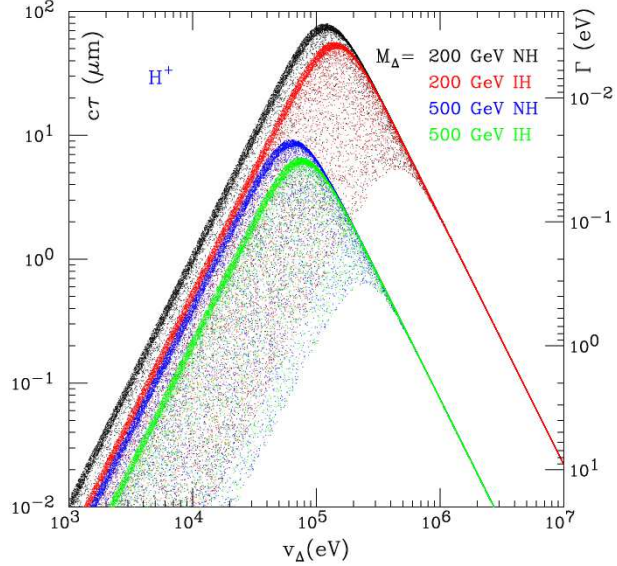
FIG. 17: Decay length and total width of the singly charged Higgs boson H^+ with $\Phi_1 = \Phi_2 = 0$.

1. Normal Hierarchy with one quasi-massless neutrino: $m_1 \approx 0$

As we have discussed in the previous section, the most important decay channels of the doubly charged Higgs are $H^{++} \to \tau^+\tau^+$, $H^{++} \to \mu^+\mu^+$ and $H^{++} \to \mu^+\tau^+$. The leading couplings, taking $s_{13} = 0$ for

TABLE I: Relations among the branching fractions of the lepton number violating Higgs decays for the neutrino mass patterns of NH, IH, and QD, with no Majorana phases $\Phi_1 = \Phi_2 = 0$.

Spectrum	Relations
Normal Hierarchy ($\Delta m_{31}^2 > 0$)	$\mathrm{BR}(H^{++} \to \tau^+\tau^+), \mathrm{BR}(H^{++} \to \mu^+\mu^+) \gg \mathrm{BR}(H^{++} \to e^+e^+)$ $\mathrm{BR}(H^{++} \to \mu^+\tau^+) \gg \mathrm{BR}(H^{++} \to e^+\mu^+), \mathrm{BR}(H^{++} \to e^+\tau^+)$ $\mathrm{BR}(H^+ \to \tau^+\bar\nu), \mathrm{BR}(H^+ \to \mu^+\bar\nu) \gg \mathrm{BR}(H^+ \to e^+\bar\nu)$
Inverted Hierarchy ($\Delta m_{31}^2 < 0$)	$\mathrm{BR}(H^{++} \to e^+e^+) > \mathrm{BR}(H^{++} \to \mu^+\mu^+), \mathrm{BR}(H^{++} \to \tau^+\tau^+)$ $\mathrm{BR}(H^{++} \to \mu^+\tau^+) \gg \mathrm{BR}(H^{++} \to e^+\tau^+), \mathrm{BR}(H^{++} \to e^+\mu^+)$ $\mathrm{BR}(H^+ \to e^+\bar\nu) > \mathrm{BR}(H^+ \to \mu^+\bar\nu), \mathrm{BR}(H^+ \to \tau^+\bar\nu)$
Quasi-Degenerate ($m_1, m_2, m_3 > |\Delta m_{31}|$)	$\mathrm{BR}(H^{++} \to e^+e^+) \sim \mathrm{BR}(H^{++} \to \mu^+\mu^+) \sim \mathrm{BR}(H^{++} \to \tau^+\tau^+) \approx 30\%$ $\mathrm{BR}(H^+ \to e^+\bar\nu) \sim \mathrm{BR}(H^+ \to \mu^+\bar\nu) \sim \mathrm{BR}(H^+ \to \tau^+\bar\nu) \approx 30\%$

simplicity, are

$$\Gamma_{++}^{22} = \frac{1}{\sqrt{2}v_\Delta}\left(\sqrt{\Delta m_{21}^2}\, c_{12}^2 c_{23}^2 + \sqrt{\Delta m_{31}^2}\, e^{-i\Phi_2} s_{23}^2\right) \tag{31}$$

$$\Gamma_{++}^{23} = \frac{s_{23}c_{23}}{\sqrt{2}v_\Delta}\left(-\sqrt{\Delta m_{21}^2}\, c_{12}^2 + \sqrt{\Delta m_{31}^2}\, e^{-i\Phi_2}\right) \tag{32}$$

$$\Gamma_{++}^{33} = \frac{1}{\sqrt{2}v_\Delta}\left(\sqrt{\Delta m_{21}^2}\, c_{12}^2 s_{23}^2 + \sqrt{\Delta m_{31}^2}\, e^{-i\Phi_2} c_{23}^2\right) \tag{33}$$

The decay rates thus depend on only one Majorana phase Φ_2. The behavior of branching fractions for all channels is shown in Fig. 18. We see the rather weak dependence of the decay branching fractions on the phase, which can be understood by realizing the large difference between the two interfering terms $\Delta m_{21} \ll \Delta m_{31}$. When the phase $\Phi_2 = \pi$, one obtains the maximal suppression (enhancement) for the channels $H^{++} \to \tau^+\tau^+$ and $H^{++} \to \mu^+\mu^+$ ($H^{++} \to \mu^+\tau^+$) by a factor of two at most.

2. Inverted Hierarchy with one quasi-massless neutrino: $m_3 \approx 0$

In the case of Inverted Hierarchy the relevant channels are $H^{++} \to e^+e^+$, $\mu^+\tau^+$, as well as $H^{++} \to e^+\mu^+$, $e^+\tau^+$. The couplings, taking $s_{13} = 0$, read as

$$\Gamma_{++}^{11} = \frac{1}{\sqrt{2}v_\Delta}\left(\sqrt{\Delta m_{21}^2 + |\Delta m_{31}^2|}\, s_{12}^2 + \sqrt{|\Delta m_{31}^2|}\, e^{-i\Phi_1} c_{12}^2\right) \approx \sqrt{\frac{|\Delta m_{31}^2|}{2v_\Delta^2}}\left(s_{12}^2 + e^{-i\Phi_1} c_{12}^2\right), \tag{34}$$

$$\Gamma_{++}^{23} = -\frac{s_{23}c_{23}}{\sqrt{2}v_\Delta}\left(\sqrt{\Delta m_{21}^2 + |\Delta m_{31}^2|}\, c_{12}^2 + \sqrt{|\Delta m_{31}^2|}\, e^{-i\Phi_1} s_{12}^2\right) \propto c_{12}^2 + e^{-i\Phi_1} s_{12}^2, \tag{35}$$

$$\Gamma_{++}^{12} = \frac{s_{12}c_{12}c_{23}}{\sqrt{2}v_\Delta}\left(-\sqrt{|\Delta m_{31}^2|}\, e^{-i\Phi_1} + \sqrt{|\Delta m_{31}^2| + \Delta m_{21}^2}\right) \propto 1 - e^{-i\Phi_1}, \tag{36}$$

$$\Gamma_{++}^{13} = \frac{s_{12}c_{12}s_{23}}{\sqrt{2}v_\Delta}\left(\sqrt{|\Delta m_{31}^2|}\, e^{-i\Phi_1} - \sqrt{|\Delta m_{31}^2| + \Delta m_{21}^2}\right) \propto -1 + e^{-i\Phi_1}. \tag{37}$$

All the relevant decays depend on only one phase Φ_1, and the cancellations due to the existence of the phase can be quite substantial as seen from the above equations. In Fig. 19 we show the dependence of the branching fractions on this Majorana phase. The maximal suppression or enhancement takes places also when $\Phi_1 = \pi$. However, in this scenario the dominant channels swap from $H^{++} \to e^+ e^+$, $\mu^+ \tau^+$ when $\Phi_1 \approx 0$ to $H^{++} \to e^+ \mu^+$, $e^+ \tau^+$ when $\Phi_1 \approx \pi$. Therefore, this qualitative change can be made use of to extract the value of the Majorana phase Φ_1.

In Figs. 20 and 21, we show the predictions of the leptonic branching fractions of the doubly charged Higgs boson for the same and different flavors versus the lightest neutrino mass and $\Phi_1 = 0$, and $\Phi_2 \in (0, 2\pi)$. These are to be compared with Figs. 13 and 14 where $\Phi_1 = \Phi_2 = 0$. Generically, the allowed ranges for the branching fractions are broadened with nonzero phases, making the BR's less predictive and it is more difficult to determine the neutrino mass pattern. For small values of the lightest neutrino mass less than 10^{-2} eV, the BR's for the NH spectrum is more spread out than that for the IH with $\Phi_2 \neq 0$ as noticed earlier. When the lightest neutrino mass is larger than 10^{-2} eV, the BR's for both the NH and the IH spectra can be further spread out.

Similar features can been seen in Figs. 22 and 23 where $\Phi_1 \in (0, 2\pi)$ and $\Phi_2 = 0$, again to be compared with Figs. 13 and 14 where $\Phi_1 = \Phi_2 = 0$. The allowed ranges for the branching fractions are broadened with nonzero phases, making the BR's less predictive. For small values of the lightest neutrino mass less than 10^{-2} eV, the BR's for the IH spectrum is more spread out than that for the NH with $\Phi_1 \neq 0$ as noticed
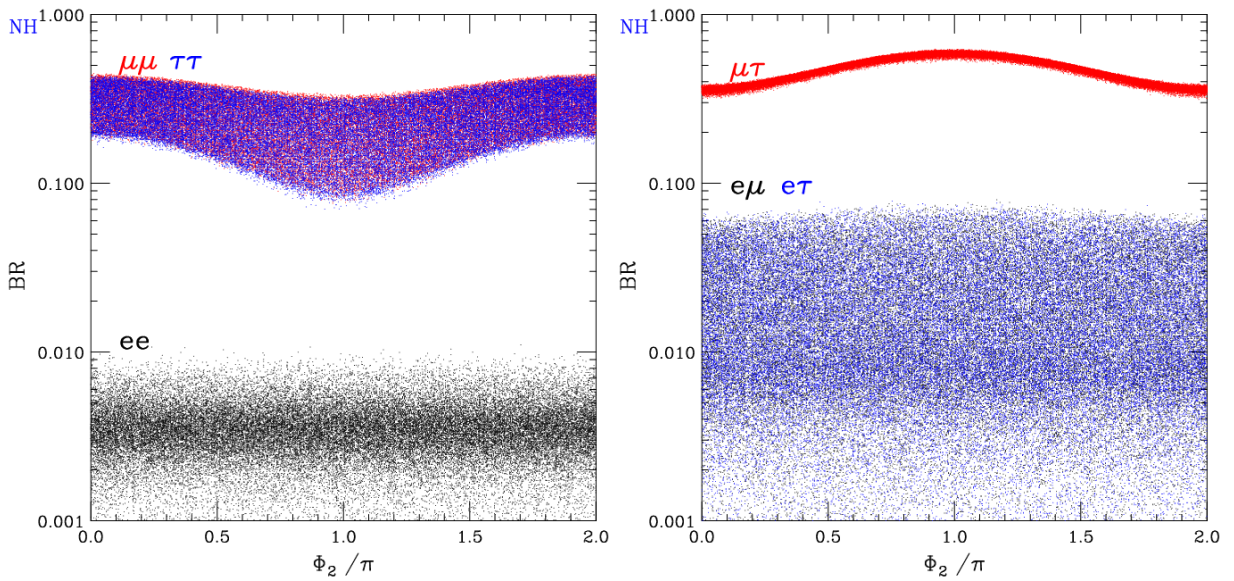

FIG. 18: Scatter plots of the same (left) and different (right) flavor leptonic branching fractions for the H^{++} decay versus the Majorana phase Φ_2 for the NH $m_1 = 0$ scenario. $\Phi_1 \in (0, 2\pi)$.
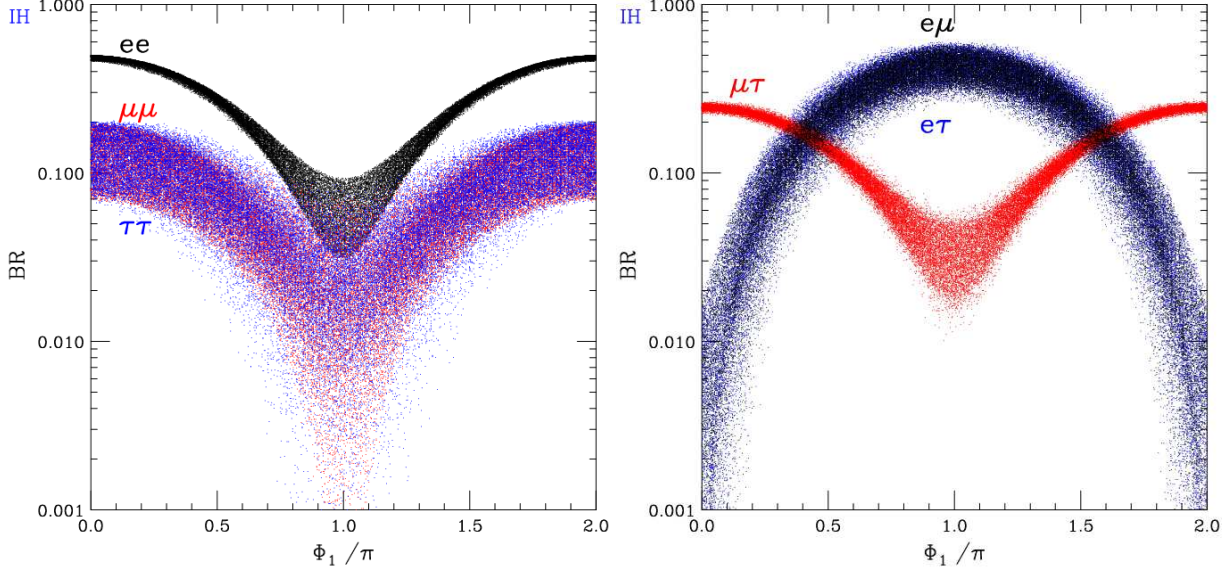
FIG. 19: Scatter plots of the same (left) and different (right) flavor leptonic branching fractions for the H^{++} decay versus the Majorana phase Φ_1 for the IH $m_3 = 0$ scenario. $\Phi_2 \in (0, 2\pi)$.
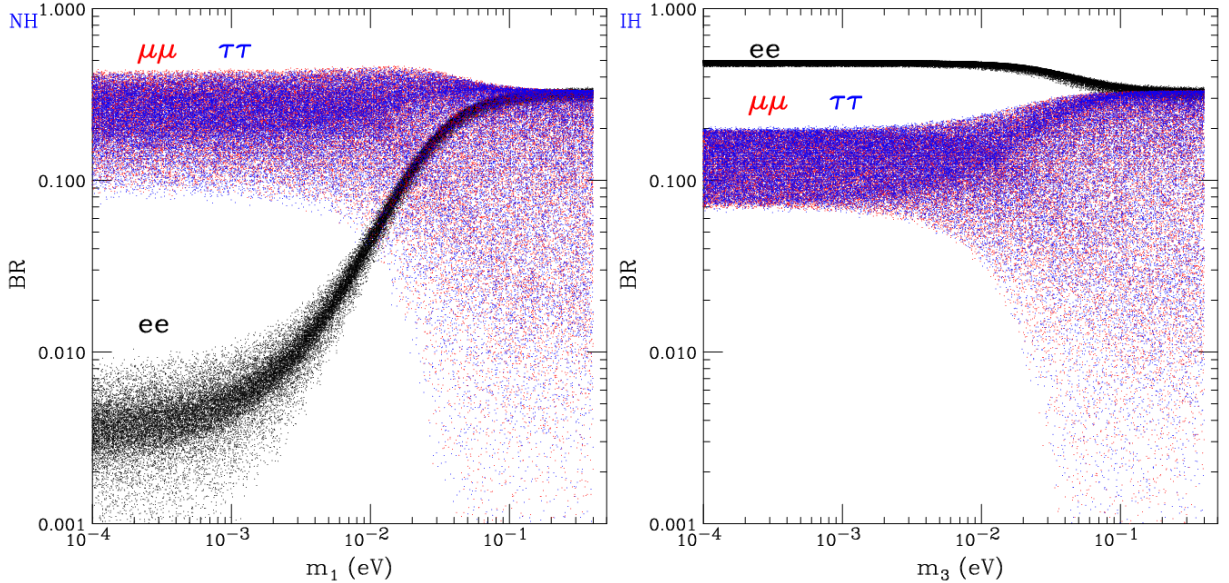
FIG. 20: Scatter plots for the H^{++} decay branching fractions to the flavor-diagonal like-sign dileptons versus the lowest neutrino mass for NH (left) and IH (right) with $\Phi_1 = 0$ and $\Phi_2 \in (0, 2\pi)$.

earlier. When the lightest neutrino mass is larger than 10^{-2} eV, the BR's for the NH can be completely spread out.

We thus conclude that the Majorana phases can change the branching fractions of the doubly charged Higgs boson dramatically. However, it is important to note that the decays of the singly charged Higgs boson $H^+ \to e_i^+ \nu$ are independent of the Majorana phases. Therefore, in order to distinguish the neutrino
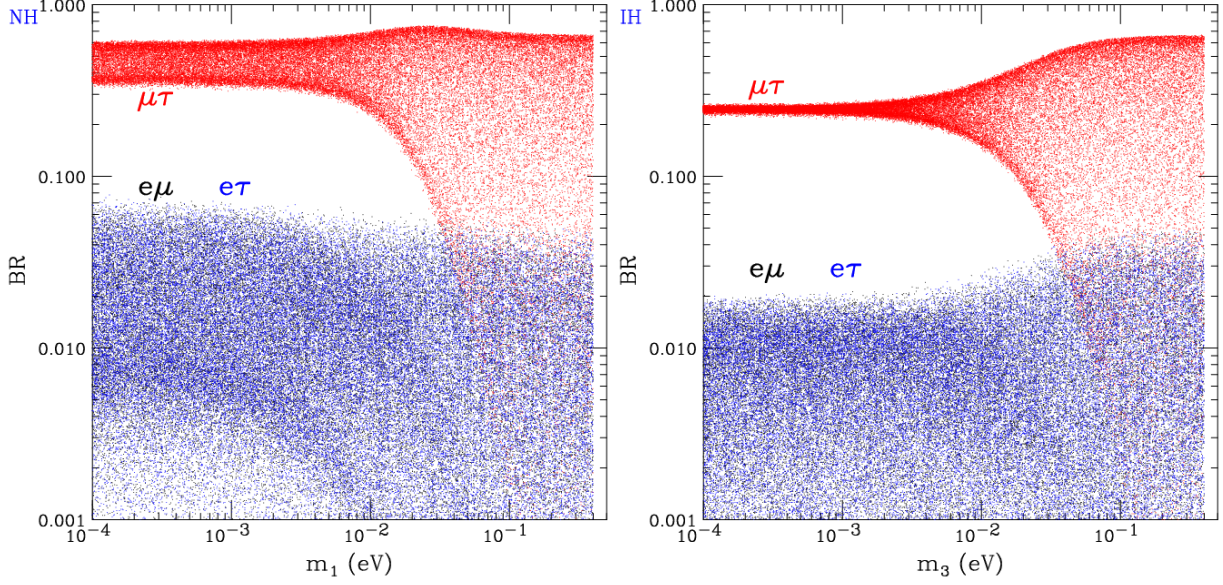
FIG. 21: Same as Fig. 20, but for H^{++} decay to the flavor-off-diagonal like-sign dileptons.
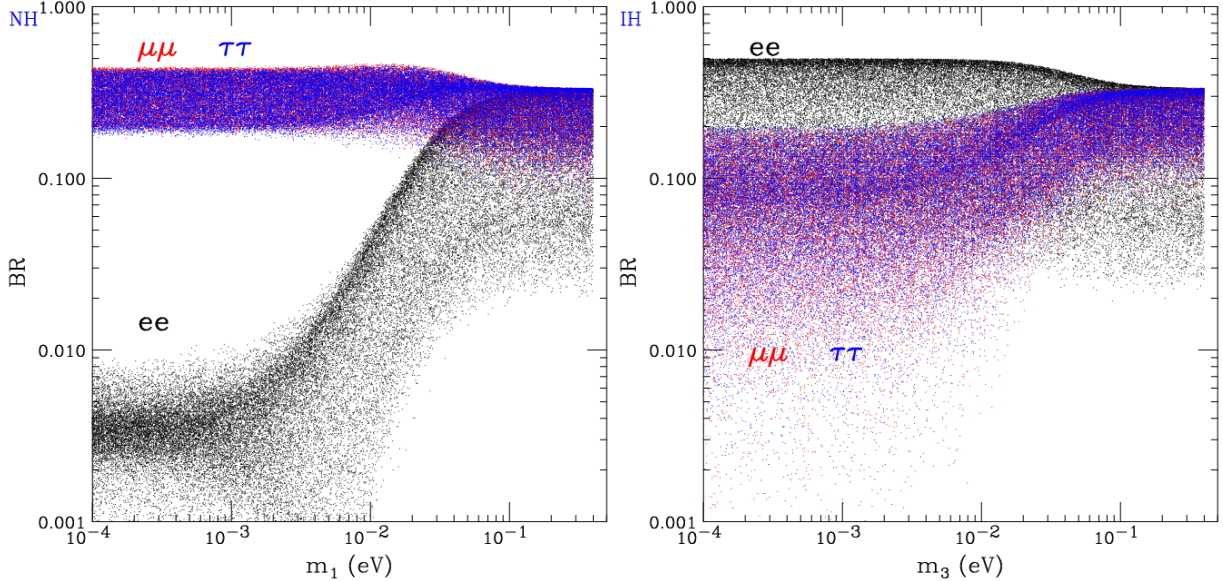
FIG. 22: Scatter plots for the H^{++} decay branching fractions to the flavor-diagonal like-sign dileptons versus the lowest neutrino mass for NH (left) and IH (right) with $\Phi_2 = 0$ and $\Phi_1 \in (0, 2\pi)$.

mass spectra non-ambiguously, it is necessary to make use of the decays of the singly charged Higgs boson. The combination of the decays of both the singly and doubly charged Higgs bosons may shed light on the Majorana phases, in particular for the sensitive dependence on Φ_1 in the case of IH.
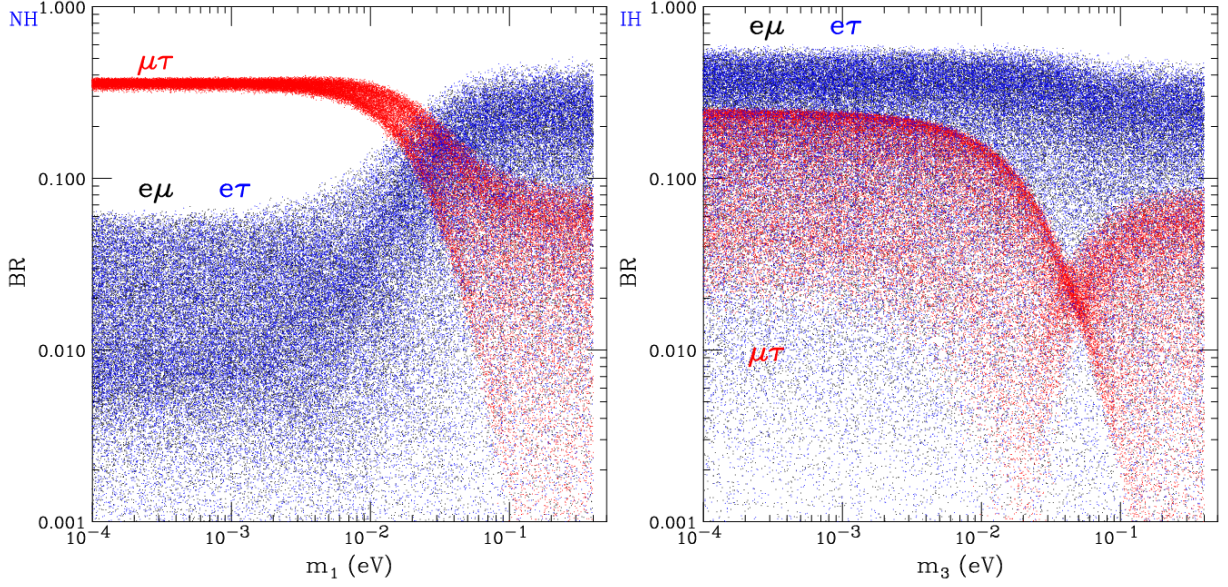
FIG. 23: Same as Fig. 22, but for H^{++} decay to the flavor-off-diagonal like-sign dileptons.

VI. SEARCHING FOR SEESAW TRIPLET HIGGS AT THE LHC

The leading production channels at hadron colliders for these Higgs bosons are the following electroweak processes:

$$q(p_1) + \bar{q}(p_2) \rightarrow H^{++}(k_1) + H^{--}(k_2)$$

$$q(p_1) + \bar{q}'(p_2) \rightarrow H^{++}(k_1) + H^{-}(k_2)$$

$$q(p_1) + \bar{q}'(p_2) \rightarrow H^{+}(k_1) + H_2(k_2)$$

In term of the polar angle variable $y = \hat{p}_1 \cdot \hat{k}_1$ in the parton c.m. frame with energy $\sqrt{s}$, the parton level cross section for these processes are

$$\frac{d\sigma}{dy}(q\bar{q} \rightarrow H^{++}H^{--}) = \frac{3\pi\alpha^2\beta_i^3(1-y^2)}{N_c s}\left\{e_q^2 + \frac{s}{(s-M_Z^2)^2}\frac{\cos 2\theta_W}{\sin^2 2\theta_W}\right.$$
$$\left. \times \left[4e_q g_V^q(s-M_Z^2) + 4(g_V^{q2}+g_A^{q2})s\frac{\cos 2\theta_W}{\sin^2 2\theta_W}\right]\right\}, \tag{38}$$

$$\frac{d\sigma}{dy}(q\bar{q}' \rightarrow H^{++}H^{-}) = 2\frac{d\sigma}{dy}(q\bar{q}' \rightarrow H^{+}H_2) = \frac{\pi\alpha^2\beta_i^3(1-y^2)}{16N_c \sin^4\theta_W}\frac{s}{(s-M_W^2)^2}, \tag{39}$$

where $\beta_i = \sqrt{(1-(m_i+m_j)^2/s)(1-(m_i-m_j)^2/s)}$ is the speed factor of H_i and H_j in the c.m. frame.

The production of $H^{\pm\pm}H^{\mp}$ [31] and $H^{\pm}H_2$ can be crucial to test its $SU(2)_L$ triplet nature at the collider. Doubly charged Higgs and singly charged Higgs can also be incorporated in other theories, for instance, the Zee-Babu model [8] where $H^{\pm\pm}$ and $H^{\pm}$ are both $SU(2)_L$ singlets, and the Majorana neutrino masses arise at two-loop level. Both pair productions of $H^{++}H^{-}$ and $H^{+}H_2$ will vanish in the Zee-Babu model
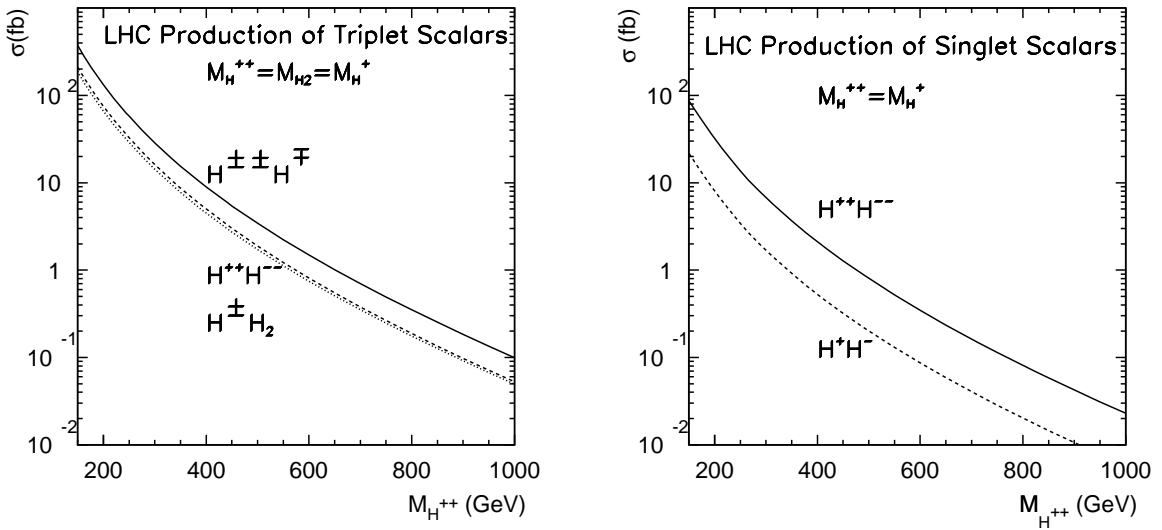
FIG. 24: Total production cross section at the LHC versus the heavy Higgs mass for (a) $H^{\pm}H_2$, $H^{\pm\pm}H^{\mp}$ and $H^{++}H^{--}$ processes in the triplet model (left), and (b) $H^{++}H^{--}$ and $H^{+}H^{-}$ processes in the singlet model (right).

due to the absence of the $SU(2)_L$ gauge couplings. Drell-Yan production of $H^{++}H^{--}$ and $H^{+}H^{-}$ will be present via the hypercharge interaction of γ and Z.

The production cross sections for all three channels are plotted in Fig. 24(a) ($H^{+}H^{-}$ is not presented since it is phenomenologically less unique and we will not study it.) For comparison, we also plot the production of $H^{++}H^{--}$ and $H^{+}H^{-}$ in Zee-Babu model in Fig. 24(b). The production rate is lower by about a factor of two comparing with the rates in the triplet model. Only tree-level results are shown in these figures. The QCD corrections to the process $H^{++}H^{--}$ have also been computed [32], and a next-to-leading (NLO) K-factor of order 1.25 at the LHC for Higgs mass range from 150 GeV to 1 TeV is predicted. QCD corrections to the production of $H^{\pm\pm}H^{\mp}$ and $H^{\pm}H_2$ are in principle very similar to $H^{++}H^{--}$ and we apply the same K-factor to these two processes in our numerical analysis. In the $H^{++}H^{--}$ production, contribution from real photon annihilation is shown [18] to be an increase of 10% to the Drell-Yan production for the above mass range at the LHC. We will apply an overall K-factor of 1.35 for the $H^{++}H^{--}$ production, and 1.25 for the $H^{++}H^{-}$ production.

A.   Purely Leptonic Modes

The light neutrino mass matrix and the leptonic decay branching fractions of triplet Higgs bosons are related by the structure of triplet Yukawa matrix Γ_{++} (or Y_{ν}). This direct correlation may enable us to test
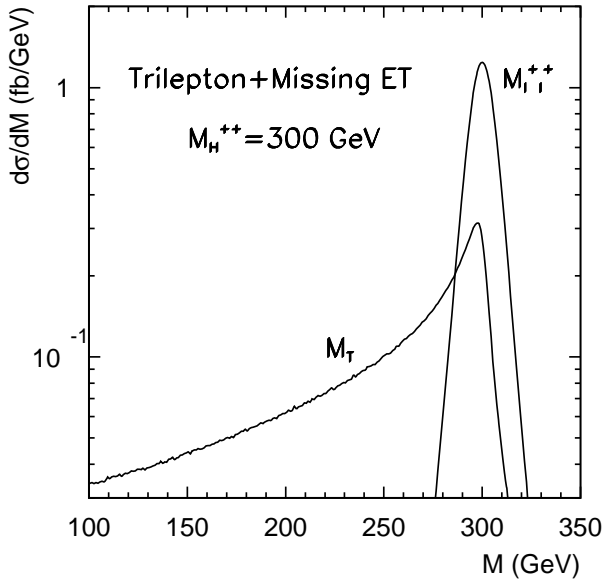
FIG. 25: Reconstructed invariant mass of $M_{\ell^\pm \ell^\pm}$ and transverse mass $M_T(\ell^\mp \nu)$ for the processes $H^{\pm\pm} H^\mp \to \ell^\pm \ell^\pm \, \ell^\mp \nu$, with a representative heavy Higgs mass 300 GeV.

the neutrino mass generation by collider observables of the decay branching fractions for different flavor combinations. Consider the case of large Yukawa couplings ($v_\Delta < 10^{-4}$ GeV), the triplet Higgs decays will be dominated by the leptonic modes

$$H^{++} \to e_i^+ e_j^+; \ \ H^+ \to e_i^+ \bar{\nu}; \ \ H_2 \to \nu\nu + \bar{\nu}\bar{\nu} \ \ (e_i = e, \mu, \tau).$$

The H_2 decays are experimentally invisible and the reconstruction of H_2 becomes impossible. Hence, we focus on the production of $H^{++} H^-$ and $H^{++} H^{--}$. In the rest of this section, we establish the observability for the leading decay channels at the LHC. We then discuss the measurement of their decay branching fractions and connect the individual channels to the neutrino mass patterns.

$$1. \ \ H^{\pm\pm} H^\mp \to \ell^\pm \ell^\pm \, \ell^\mp \nu \ \ (\ell = e, \mu)$$

We start from the easy channels with e, μ in the final state of the Higgs decays. The signal consists of one pair of same sign leptons and another opposite sign lepton plus missing energy. We employ the following basic acceptance cuts for the event selection [33]

$$p_T(\ell_{\mathrm{hard}}) > 30 \text{ GeV}, \ \ p_T(\ell) > 15 \text{ GeV}, \ \ \not{E}_T > 40 \text{ GeV},$$

$$|\eta(\ell)| < 2.5, \ \ \Delta R_{\ell\ell} > 0.4. \tag{40}$$
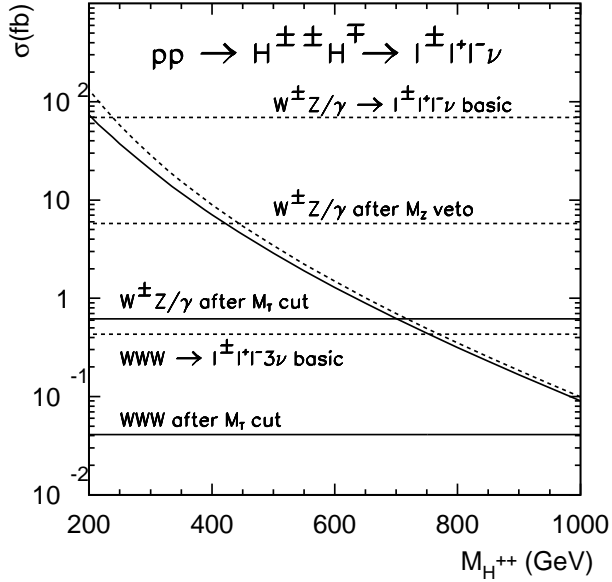
FIG. 26: Production cross section of $H^{\pm\pm}H^{\mp} \to \ell^{\pm}\ell^{\pm}\, \ell^{\mp}\nu$ at the LHC versus the heavy Higgs mass with (solid curve) and without (dashed curve) the kinematical cuts. Branching fractions for the Higgs decays are taken to be 100% for illustration. For comparison, the background processes are also included with the sequential cuts as indicated.

To simulate the detector effects on the energy-momentum measurements, we smear the electromagnetic energy and the muon momentum by a Gaussian distribution whose width is parameterized as [33]

$$\frac{\Delta E}{E} \;=\; \frac{a_{cal}}{\sqrt{E/\text{GeV}}} \oplus b_{cal}, \quad a_{cal} = 5\%, \; b_{cal} = 0.55\%, \tag{41}$$

$$\frac{\Delta p_T}{p_T} \;=\; \frac{a_{track}\, p_T}{\text{TeV}} \oplus \frac{b_{track}}{\sqrt{\sin\theta}}, \quad a_{track} = 15\%, \; b_{track} = 0.5\%. \tag{42}$$

For high p_T leptons, the electromagnetic energy resolution is better than muon's tracking resolution.

The irreducible SM backgrounds to this channel are

$$W^{\pm}Z/\gamma^* \to \ell^{\pm}\nu\ell^+\ell^-, \;\; W^{\pm}W^{\pm}W^{\mp} \to \ell^{\pm}\ell^+\ell^- + \not{E}_T.$$

Although the backgrounds are quite sizable with the basic leptonic cuts, the order of 100 fb for WZ and 1 fb for WWW, the kinematics is very different between the signal and the backgrounds. We outline the characteristics and propose some judicious cuts as follows.

- To remove the WZ background, we veto the lepton pairs with the same flavor but opposite charges in the Z-mass window $|M_{\ell^+\ell^-} - M_Z| > 15$ GeV.

- The mass reconstruction for $\ell^{\pm}\ell^{\pm}$ and $\ell^{\mp}\nu$ can be very indicative. We first define a transverse mass M_T by the opposite sign lepton and missing transverse energy

$$M_T(\ell^{\mp}\nu) = \sqrt{(E_T(\ell) + \rlap{/}{E}_T)^2 - (\vec{p}_T(\ell) + \vec{\rlap{/}{p}}_T)^2}.$$

  This variable and the invariant mass of the like-sign dileptons are plotted in Fig. 25. We then impose a modest cut

$$M_T > 200 \text{ GeV}. \tag{43}$$

  The cut can be further tightened up for heavier Higgs searches.

- Finally, when we perform the signal significance analysis, we look for the resonance in the mass distribution of $\ell^+\ell^+$. For instance, if we look at a mass window of $M_\Delta \pm 25$ GeV in $M_{\ell^+\ell^+}$, the backgrounds will be at a negligible level.

The production cross section of $H^{\pm\pm}H^{\mp} \to \ell^{\pm}\ell^{\pm}\,\ell^{\mp}\nu$ with (solid curve) and without (dashed curve) the kinematical cuts are plotted in Fig. 26. Branching fractions for the Higgs decays are taken to be 100% for illustration. For comparison, the background processes of WZ and WWW are also included with the sequential cuts as indicated. The backgrounds are suppressed substantially.

As a remark, we would like to comment on the other potentially large, but reducible backgrounds, the heavy quark production such as $t\bar{t}$, $Wb\bar{b}$ etc. The $t\bar{t}$ production rate is very high, leading to the $\ell^+\ell^-\,X$ final state with about 40 pb. Demanding another isolated lepton presumably from the b quarks and with the basic cuts, the background rate will be reduced by about three to four orders of magnitude. The stringent lepton isolation cut for multiple charged leptons can substantially remove the b-quark cascade decays. With the additional M_T and $M_{\ell^+\ell^+}$ cuts, the backgrounds should be under control.

$$2. \quad H^{\pm\pm}H^{\mp} \to \ell^{\pm}\ell^{\pm}\,\tau^{\mp}\nu \quad (\ell = e, \mu)$$

The τ-lepton final state from $H^{\pm\pm}$ or $H^{\pm}$ decay plays an important role in distinguishing different patterns of light neutrino masses. Its identification and reconstruction are different from e, μ final states. There will always be a missing ν_τ associated with the τ decay, and there is also a missing neutrino from H^+ decay as well. If the missing neutrinos are all from the same Higgs parent, one can still construct this Higgs boson via the transverse mass variable. However, if the τ is from another Higgs decay like the $H^{\pm\pm}$, the reconstruction will be difficult due to the multiple neutrinos from different parents. Therefore in this section, we select the event involving a τ final state only from the decay $H^{\pm} \to \tau^{\pm}\nu$.

	$M_{H^+} = 300$ GeV			$M_{H^+} = 600$ GeV		
p_T^ℓ threshold (GeV)	50	75	100	100	150	200
ℓ misidentification rate	2.9%	9.4%	17.6%	4.6%	12.4%	22.2%
τ survival probability	57.0%	69.8%	78.8%	62.8%	75.7%	83.7%

TABLE II: The misidentified rate of τ from $H^\pm \to e\nu, \mu\nu$ and the survival probability for $\tau \to e\nu\nu$, $\mu\nu\nu$ in the channels $H^{\pm\pm}H^\mp \to \ell^\pm\ell^\pm \tau^\mp\nu$.

Besides the two like-sign leptons that reconstruct the $H^{\pm\pm}$ and are selected based on the basic cuts Eq. (40), we need to adjust the threshold for the τ decay products that are significantly softer than the direct decay from a heavy Higgs boson. We accept isolated charged tracks as τ candidates (the "1-prong" and "3-prong" modes). For the muons and the other charged tracks, we take

$$p_T(\mu) > 5 \text{ GeV}, \quad p_T(\text{track}) > 10 \text{ GeV}.$$

With further kinematical selection similar to the last section, the irreducible SM background is well under control. There may be additional backgrounds with a jet to fake a τ, such as $W^\pm W^\pm jj$. According to ATLAS TDR [34], for a hard τ in the range of $p_T \sim 70 - 130$ GeV, where τ identification efficiency is 60%, the jet faking rate is 1% into a hadronic decaying τ. Knowing the cross section for $W^\pm W^\pm jj$ is the order of 15 fb after the basic cuts, this leads to a faked background cross section to be way below 0.1 fb, after vetoing the extra jet before the Higgs mass reconstruction.

There is one more complication for the event selection for the leptonic modes. In order to identify the τ flavor, we must know if the e or μ is from a τ decay or from a heavy Higgs decay. Once again, we make use of the fact that the lepton from a τ decay is softer. We simulate the events and examine the fraction of wrong and correct τ identification with a given p_T threshold and the results are presented in Table II. If an event contains a lepton with p_T less than the values shown in the table, it will be identified as τ leptonic decay. Table II gives the misidentification rate of τ from $H^\pm \to e\nu, \mu\nu$ and the survival probability for $\tau \to e\nu\nu$, $\mu\nu\nu$. To effectively keep the τ events, we choose in the rest of the analysis the threshold $p_T < 100$ GeV for $M_{H^+} = 300$ GeV and $p_T < 200$ GeV for $M_{H^+} = 600$ GeV.

3. $H^{++}H^{--} \to \ell^+\ell^+ \ell^-\tau^-, \quad \ell^+\ell^+ \tau^-\tau^-, \quad \ell^+\tau^+ \ell^-\tau^-, \quad \ell^+\tau^+ \tau^-\tau^-$

The best channels for $H^{++}H^{--} \to \ell^+\ell^+\ell^-\ell^-$ ($\ell = e, \mu$) have been discussed extensively in the literature [18]. However, it has been strongly motivated in the early sections to look for channels with τ's in the final state, such as $H^{++} \to e^+\tau^+, \mu^+\tau^+, \tau^+\tau^+$. Identifying decays of doubly charged Higgs bosons with τ final state is crucial to distinguish different spectra of the neutrino mass.
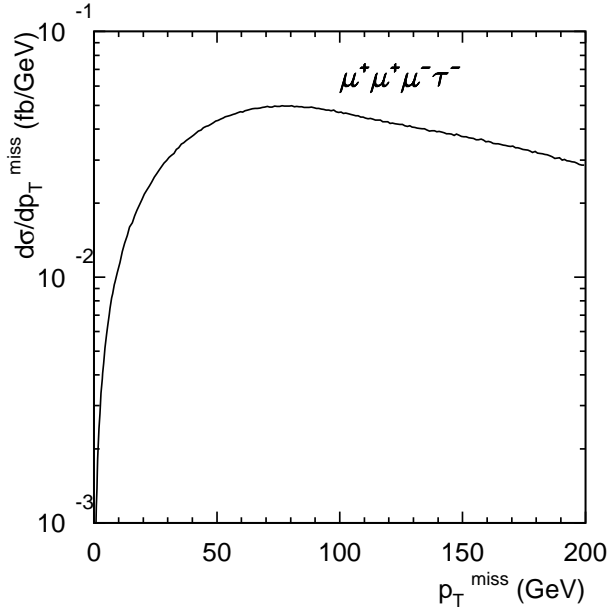
FIG. 27: $\not{p}_T$ distribution in the channel $H^{++}H^{--} \to \mu^+\mu^+\mu^-\tau^-$ with $\tau \to \ell\nu\bar{\nu}$ for $M_{H^{++}} = 300$ GeV.

For signals with neutrinos only from τ decays, the $\not{p}_T$ spectrum will be softer. This is shown in Fig. 27 for events of $\mu^+\mu^+\mu^-\tau^-$. Given the clean leptonic final state, we thus adjust the $\not{p}_T$ cut as

$$\not{p}_T > 20 \text{ GeV}. \tag{44}$$

It is important to carefully consider the kinematical reconstruction of the events with τ's. First of all, we note that all the τ's are very energetic, coming from the decay of a heavy Higgs boson. For events with one τ and no other sources for missing particles, the missing momentum will be along the direction with the charged track. We thus have

$$\vec{p}\,(\text{invisible}) = k\vec{p}\,(\text{track}), \tag{45}$$

where the proportionality constant k is determined from the $\not{p}_T$ measurement by assigning $\not{p}_T = kp_T(\text{track})$. For events with two τ's, we generalize it to

$$\vec{p}\,(\text{invisible}) = k_1\vec{p}\,(\text{track}_1) + k_2\vec{p}\,(\text{track}_2). \tag{46}$$

As long as the two τ tracks are not linearly dependent, k_1 and k_2 can be determined again from the $\not{p}_T$ measurement. The Higgs pair kinematics is thus fully reconstructed. In practice, we require that the invisible momenta pair with the two softer leptons to solve the combinatorics of the multiple charged leptons. The Higgs masses reconstructed from the like-sign dileptons are shown in Fig. 28 for the process $H^{++}H^{--} \to \mu^+\mu^+\tau^-\tau^-$. It is clear that the $\mu\mu$ mass reconstruction has a better resolution than the $\tau\tau$ pair.
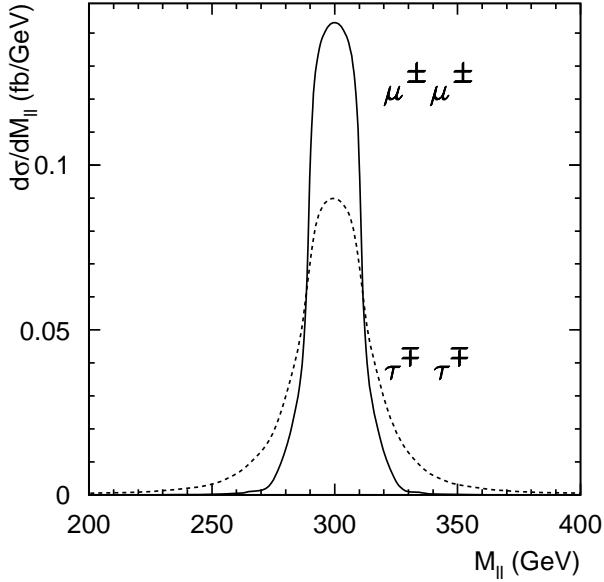
FIG. 28: Reconstructed invariant mass distributions for the like-sign $\mu\mu$ (solid) and $\tau\tau$ (dotted) in $H^{++}H^{--} \rightarrow \mu^+\mu^+ \tau^-\tau^-$ for $M_{H^{++}} = 300$ GeV.

One of the main features for the Higgs pair production is the equal heavy mass in the final state, $M_{\ell^+\ell^+} = M_{\ell^-\ell^-}$ for the doubly charged Higgs production. This serves as an important discriminator for the signal selection against the backgrounds. This can also be used for momentum reconstruction with an additional τ. As long as we have less than 3 unknowns, we will be able to determine the solutions. This extends the final states to contain up to three τ's, such as $\ell^+\tau^+ \tau^-\tau^-$ [17].

If the final state involves leptons plus one τ (e.g., $\ell^+\ell^+\ell^-\tau^-$) with τ hadronic decay, the SM background will be $W^\pm Z+j$ and $W^\pm W^\pm W^\mp +j$. As shown in last section, $W^\pm Z$ and $W^\pm W^\pm W^\mp$ is below 1 fb after imposing M_Z veto. With additional jet in final state and multiplied the rate of jet fake hadronic τ which is 1%. It will be of the order $\mathcal{O}(10^{-3})$ fb and negligible. This remains true for events with two or more τs. For instance, $\ell^+\ell^+\tau^-\tau^-$ may encounter W^+W^+jj background, but the rate for both jets to fake hadronic τ's is $(1\%)^2$, resulting in a background rate about 10^{-3} fb with basic cuts. As for the other reducible background, the QCD $t\bar{t}$ production, we expect that the combination of the small fake rate of $b \rightarrow \ell, \tau$ and effective kinematical cuts on $M_T, M_{\ell^\pm\ell^\pm}$ would be sufficient to bring the faked background to a low level.
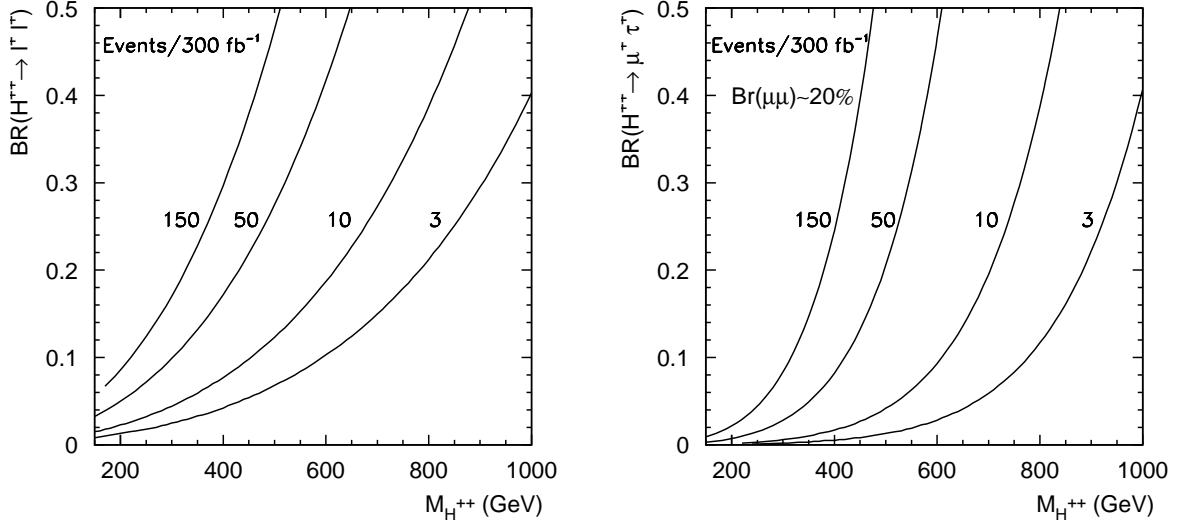
FIG. 29: Event contours in the BR$-M_{H^{++}}$ plane for the doubly charged Higgs decay at the LHC with an integrated luminosity 300 fb^{-1} for $\mu^+\mu^+\mu^-\mu^-$ (left) and for $\mu^+\mu^+\mu^-\tau^-$ (right), assuming BR($H^{++} \to \mu^+\mu^+$) = 20%.

4. Measuring Branching Fractions and Probing the Neutrino Mass Pattern

The direct correlation between leptonic branching fractions of triplet Higgs decay and realistic light neutrino mass matrix is central for the Type II seesaw predictions. Measuring the BR's of different flavor combinations becomes very crucial here. For illustration, consider the cleanest channel with four muons first, $H^{++}H^{--} \to \mu^+\mu^+\mu^-\mu^-$. The event rate is written as

$$N_{4\mu} = L \times \sigma(pp \to H^{++}H^{--}) \times \text{BR}^2(H^{++} \to \mu^+\mu^+), \tag{47}$$

where L is the integrated luminosity. Given a sufficient number of events N, the mass of doubly charged Higgs boson is determined by the invariant mass of the like-sign muons $M_{\mu^+\mu^+}$. We thus predict the corresponding production rate $\sigma(pp \to H^{++}H^{--})$ for this given mass. The only unknown in the Eq. (47) is the decay branching fraction.

This procedure can be applicable for any channels that have been discussed for full reconstruction earlier. In the Type II seesaw scheme, we have BR($H^{++} \to \mu^+\mu^+$) $\sim 20 - 40\%$ for both NH and IH patterns as seen in Sec. V. Once we have measured this BR($\mu^+\mu^+$), we can use it to determine other channels, such BR($H^{++} \to \mu^+\tau^+$, $\tau^+\tau^+$) and BR($H^+ \to \tau^+\bar{\nu}$).

With negligible SM backgrounds, the only limitation would be the event rate that determines the statistical error for the BR measurements, $i.$ $e.$, a relative error $1/\sqrt{N}$ if Gaussian statistics is applicable. We present the event contours in the BR$-M_{H^{++}}$ plane in Fig. 29 for 300 fb^{-1}.

Signal channels	Leading modes and BR range Normal Hierarchy	Leading modes and BR range Inverted Hierarchy
$H^{++}H^{--}$		
$\Phi_1 = \Phi_2 = 0$	$\mu^+\mu^+ \ \mu^-\mu^- \quad (20-40\%)^2$	$e^+e^+ \ e^-e^- \quad (50\%)^2$
	$\mu^+\mu^+ \ \mu^-\tau^- \quad (20-40\%) \times 35\%$	$e^+e^+ \ \mu^-\tau^- \quad 50\% \times 25\%$
	$\mu^+\mu^+ \ \tau^-\tau^- \quad (20-40\%)^2$	$\mu^+\tau^+ \ \mu^-\tau^- \quad (25\%)^2$
	$\mu^+\tau^+ \ \mu^-\tau^- \quad (35\%)^2$	
	$\mu^+\tau^+ \ \tau^-\tau^- \quad 35\% \times (20-40\%)$	
$\Phi_1 \approx \pi, \ \Phi_2 = 0$	same as above	$ee, \mu\tau \to e\mu, e\tau \quad (30-60\%)^2$
$\Phi_1 = 0, \ \Phi_2 \approx \pi$	$\mu\mu, \tau\tau : \times 1/2, \ \mu\tau : \times 2$	same as above
$H^{\pm\pm}H^{\mp}$		
$\Phi_1 = \Phi_2 = 0$	$\mu^+\mu^+ \ \mu^-\nu \quad (20-40\%) \times (35-60\%)$	$e^+e^+ \ e^-\nu \quad (50\%)^2$
	$\mu^+\mu^+ \ \tau^-\nu \quad (20-40\%) \times (35-60\%)$	
$\Phi_1 \approx \pi, \ \Phi_2 = 0$	same as above	$ee \to e\mu, e\tau \quad (30-60\%) \times 50\%$
$\Phi_1 = 0, \ \Phi_2 \approx \pi$	$\mu\mu : \times 1/2$	same as above

TABLE III: Leading fully reconstructable leptonic channels and the indicative ranges of their branching fractions for $v_\Delta \lesssim 10^{-4}$ GeV. The light neutrino mass patterns of the NH and IH, as well as vanishing and large Majorana phases are compared.

To summarize our signal reconstruction in this section, we list the leading reconstructable leptonic channels along with the branching fractions in Tabel III. We also associate these channels with predictions of the neutrino mass patterns. These channels are not very sensitive to the Majorana phase Φ_2, and the maximal variation in the branching fractions can be up to a factor of 2 in the case of NH. The sensitivity to Φ_1 can be very significant in the case of the IH. As for the case of quasi-degenerate spectrum, the Higgs decay branching fractions for the three flavors of e, μ, τ are equally distributed as given in Table I, while the off-diagonal channels are negligibly small.

B. Gauge Boson Decay Modes

Although the triplet vev is constrained from above by the ρ-parameter at the order of a GeV or so, the pure gauge boson channel can still become dominant even for rather small values of the triplet vev, *i.e.* $v_\Delta > \mathcal{O}(10^{-4}$ GeV$)$, especially for increasing the triplet mass. In this limit, the triplet Higgs bosons will decay dominantly to the SM gauge boson pairs as discussed in the early sections. Unfortunately, the absence of lepton number violation decays would prevent us from extracting any information of neutrino mass patterns. However, we would like to emphasize that the μ-term in Eq. (4) has the identical gauge structure
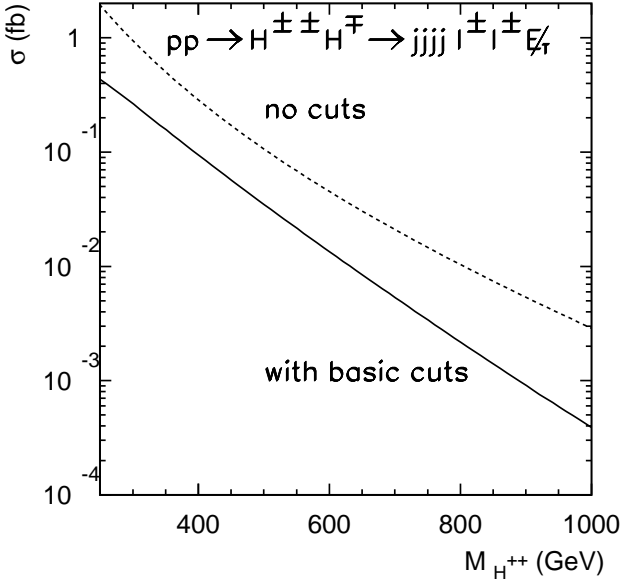
FIG. 30: Total cross section for $H^{\pm\pm}H^{\mp} \to jjb\bar{b}\ell^+\ell^+\not{E}_T$ at the LHC versus the heavy Higgs mass before (dotted curve) and after the basic cuts (solid).

of the interactions as the Majorana mass generation in Eq. (3). We therefore argue that confirmation of the existence of the Higgs triplet mixing with the SM doublets would strongly indicate the Majorana mass generation to be at work.

Collider searches for $pp \to H^{++}H^{--} \to W^+W^+W^-W^-$ has been studied before [18]. While the $W^{\pm}W^{\pm}$ channels are unique for the signal identification, we would like to search for channels that confirm the mixing between the Higgs triplet and the SM doublets. These include the decays via the following channels directly proportional to μ

$$H^+ \to W^+H_1, \ t\bar{b}, \quad H_2 \to H_1H_1, \quad A \to H_1Z, \tag{48}$$

and those proportional to a combination of μ and v_{Δ},

$$H^+ \to W^+Z, \quad H_2 \to W^+W^-, \ ZZ. \tag{49}$$

Both $H^{\pm}H_2$ and $H^{\pm\pm}H^{\mp}$ production channels are crucial to test $SU(2)_L$ gauge coupling and confirm the triplet nature of the Higgs fields. However, it would be very challenging to study the channel $H^+H_2 \to W^+H_1H_1H_1$, which consists 6 b-jets + $W^{\pm}$. The reconstruction of three light Higgs bosons from the multiple b jets would suffer from combinatorics, along with the irreducible QCD backgrounds. We will thus focus on $H^{\pm\pm}H^{\mp}$ for our study. We propose to reconstruct the events by looking for two like-sign

$W^{\pm}$'s from $H^{\pm\pm}$ decay through a pair of like-sign dileptons; the $W^{\mp}$ in their hadronic decay modes and the SM-like Higgs $H_1 \to b\bar{b}$, both from $H^{\mp}$ decay,

$$pp \to H^{\pm\pm}H^{\mp} \to W^{\pm}W^{\pm} + W^{\mp}H_1/W^{\mp}Z/\bar{t}b(t\bar{b}) \to jj\, b\bar{b}\, \ell^{\pm}\ell^{\pm}\not{E}_T. \tag{50}$$

The decay branching fractions to final states are, respectively,

$$\mathrm{BR}(W^{\pm}W^{\pm}, W^{\mp}H_1) \sim 2.2\%, \quad \mathrm{BR}(W^{\pm}W^{\pm}, W^{\mp}Z) \sim 2.3\%, \quad \mathrm{BR}(W^{\pm}W^{\pm}, \bar{t}b/t\bar{b}) \sim 3.3\%. \tag{51}$$

For a M_{H_1} of 120 GeV, the $\mathrm{BR}(H_1 \to b\bar{b})$ is about 67.7%. The decay branching fraction of the singly charged Higgs boson needs to be included as given in Fig. 8(a).

We again start with some basic cuts. We demand

$$p_T(\ell) \geq 15 \text{ GeV}, \quad |\eta(\ell)| \leq 2.5, \quad \not{E}_T > 30 \text{ GeV}, \tag{52}$$

$$p_T(j) \geq 25 \text{ GeV}, \quad |\eta(j)| \leq 3.0, \quad \Delta R_{jj},\ \Delta R_{j\ell},\ \Delta R_{\ell\ell} > 0.4. \tag{53}$$

The jet energies are also smeared using the same Gaussian formula as in Eq. (41), but with [33]

$$a = 100\%, \quad b = 5\%. \tag{54}$$

We show the total cross section for the inclusive process $H^{\pm\pm}H^{\mp} \to jjb\bar{b}\ell^{\pm}\ell^{\pm}\not{E}_T$ in Fig. 30 without any cuts (dotted curve) and after the basic cuts (solid curve). We see that with the branching fractions included, the signal rate becomes rather low.

The leading irreducible background to our signal is

$$pp \to t\bar{t}W^{\pm} \to jj\, b\bar{b}\, W^{\pm}W^{\pm}. \tag{55}$$

The QCD $jjjj + W^{\pm}W^{\pm}$ is much smaller. This is estimated based on the fact that QCD $jjW^{\pm}W^{\pm} \to jj\ell^{\pm}\ell^{\pm}\not{E}_T$ is about 15 fb. With an additional α_s^2 and 6 body phase space suppression, it is much smaller than $t\bar{t}W^{\pm}$. To maximally retain the signal rate, we will not demand the b tagging. Instead, we tighten up the kinematical cuts

$$p_T^{max}(\ell) > 50 \text{ GeV}, \quad p_T^{max}(j) > 100 \text{ GeV}. \tag{56}$$

Furthermore, for pair production of heavy particles like the two triplet Higgs bosons of several hundred GeV, the cluster mass of the system indicates the large threshold. We define

$$M_{cluster} = \sqrt{M_{4j}^2 + (\textstyle\sum \vec{p_T}^j)^2} + \sqrt{M_{\ell\ell}^2 + (\textstyle\sum \vec{p_T}^{\ell})^2} + \not{E}_T \tag{57}$$
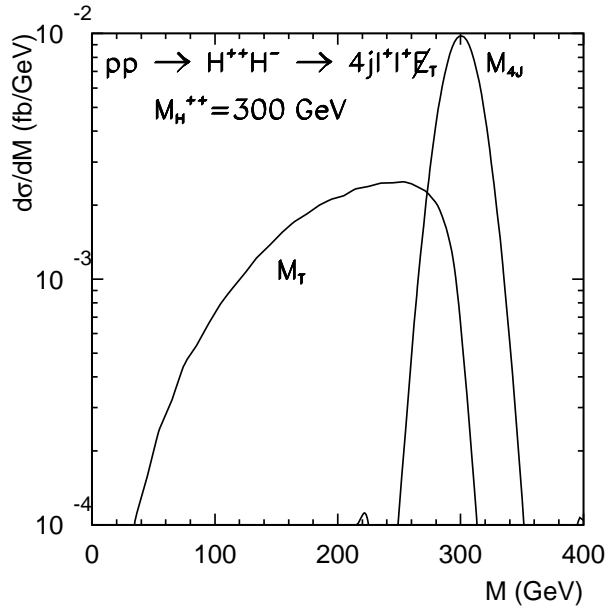
FIG. 31: Reconstruction of triplet Higgs bosons via 4-jet invariant mass M_{jjjj} for $H^{\pm}$ and transverse mass M_T for $H^{\pm\pm}$ with $M_{H^{++}} = 300$ GeV.

and will impose a high mass cut to select the signal events. With W^+H_1, W^+Z, $t\bar{b}$ and W^+W^+ all decay hadronically, we consider the mass reconstruction by the di-jets. We first impose a cut

$$|M_{jj}^W - M_W| < 15 \text{ GeV}, \tag{58}$$

where M_{jj}^W is the jet mass of six combinatorics that is closest to M_W. The second reconstruction of M_{jj} will give us the separation of M_W, M_Z, or M_{H_1}.

The singly charged triplet $H^{\pm}$ decay has no missing particles and we can fully reconstruct the $H^{\pm}$ by form a 4-jet invariant mass M_{jjjj}. The doubly charged Higgs, on the other hand, gives two like-sign dileptons plus large missing energy. We define the leptonic transverse mass

$$M_T = \sqrt{(\sqrt{M_{\ell\ell}^2 + (\sum \vec{p_T}^{\ell})^2} + \not{E}_T)^2 - (\sum \vec{p_T}^{\ell} + \vec{\not{E}}_T)^2}. \tag{59}$$

These two variables are plotted in Fig. 31 for $M_{H^{++}} = 300$ GeV.

In the leading background $t\bar{t}W$, there is another top quark that decays leptonically. Taking the b-jet left over from the three jets of m_t reconstruction, we can construct two $M_{b\ell_1}$ and $M_{b\ell_2}$. If both b and ℓ come from the same top quark, there will be a strict constraint $M_{b\ell} < m_t$. However, this cut will also reduce the signal by 70%. The wrong pair of $M_{b\ell}$ will be smaller in the $t\bar{t}W$ case since the b and ℓ are both softer than

σ (fb) cuts	Basic Cuts	p_T^ℓ cut > 50 GeV	p_T^j cut > 100 GeV	$M_{\rm Cluster}$ > 600 GeV	M_W rec. $M_W \pm 15$ GeV	M_X rec. or M_t veto	M_T < 300 GeV	M_{jjjj} 300 $\pm$ 50 GeV
$t\bar{b}$	0.13	0.12	0.12	0.11	0.11	0.094*	0.094	0.092
WH	0.074	0.069	0.065	0.061	0.06	0.046	0.045	0.045
WZ	0.06	0.056	0.053	0.05	0.05	0.038	0.038	0.038
$H^{\pm\pm}H^{\mp}$ sum	0.26	0.25	0.24	0.22	0.22	0.18	0.18	0.17
$H^{\pm\pm}H^{\mp\mp}$	0.24	0.23	0.22	0.21	0.21	0.18	0.17	0.17
$t\bar{t}W$	3.1	2.5	1.8	1.4	1.4	0.88*	0.52	0.095
					(M_{H_1} rec.$\rightarrow$)	0.15	0.097	0.045
					(M_Z rec.$\rightarrow$)	0.11	0.071	0.032
					(M_W rec.$\rightarrow$)	0.096	0.06	0.026

TABLE IV: Production cross sections (in fb) at the LHC for $pp \to H^{\pm\pm}H^{\mp} \to W^{\pm}W^{\pm}W^{\mp}H_1/W^{\pm}W^{\pm}W^{\mp}Z^0 \to jjjj+\ell^{\pm}\ell^{\pm}+\not{E}_T$ and $pp \to H^{++}H^{--} \to W^+W^+W^-W^- \to jjjj+\ell^{\pm}\ell^{\pm}+\not{E}_T$, and for the leading backgrounds. We take $M_{H^{\pm\pm}} = M_{H^{\pm}} = 300$ GeV for illustration. The rates after imposing each selection criterion, as described in the text, are shown.

the signal. We impose a cut

$$M_{b\ell}^{\rm max} > 150 \text{ GeV}. \tag{60}$$

We show the effects of the cuts step by step in Table IV for both the signal with $M_{H^{++}} = 300$ GeV and the leading background $t\bar{t}W$. We combine the four decay channels in the table. We see that all the cuts designed here are highly efficient in retaining the signal and suppressing the background. One can reach a signal to background ratio of $2:1$ and about 50 signal events/300 fb^{-1}.

For heavier Higgs bosons, the gauge boson decay modes of the singly charged Higgs boson take over the $t\bar{b}$ mode. As an illustration, for $M_{H^+} = M_{H^{++}} = 600$ GeV, the $H^+ \to t\bar{b}$ is only 18% so we don't include this channel. Another important difference for a heavier Higgs boson is that the W, Z, top and H_1 from $H^{\pm}$ decay become energetic and their decay products will be highly collimated. The signal thus may look like

$$pp \to H^{\pm\pm}H^{\mp}, \; H^{\pm\pm}H^{\mp\mp} \to W^{\pm}W^{\pm}JJ \to JJ + \ell^{\pm}\ell^{\pm} + \not{E}_T, \tag{61}$$

where J denotes a massive fat jet.

We note that the main source of the background is from $W^{\pm}W^{\pm}+$QCD jets. A light jet develops finite mass due to the QCD radiation and parton showering. Although it is difficult to accurately quantify a jet mass, we parameterize a jet mass as a function of its transverse energy $M_J \simeq 15\% E_T^J$, and require the jet mass to reconstruct M_W and M_X ($X = H_1, Z, W$).

σ (fb) cuts	Basic Cuts	p_T^ℓ cut > 80 GeV	p_T^j cut > 200 GeV	M_{J_1} rec. $M_W \pm 15$ GeV	M_{J_2} rec. $M_X \pm 15$ GeV	M_{JJ} 600 ± 75 GeV
WH	1.1×10^{-2}	9.5×10^{-3}	9.5×10^{-3}	9.4×10^{-3}	9.1×10^{-3}	9.0×10^{-3}
WZ	1.0×10^{-2}	1.0×10^{-2}	1.0×10^{-2}	1.0×10^{-2}	9.9×10^{-3}	9.8×10^{-3}
$H^{\pm\pm}H^{\mp\mp}$	3.3×10^{-2}	3.2×10^{-2}	3.1×10^{-2}	3.1×10^{-2}	3.1×10^{-2}	3.1×10^{-2}
$JJW^{\pm}W^{\pm}$	14.95	7. 65	4.69	0.24		
				(M_{H_1} rec.$\rightarrow$)	6×10^{-2}	4.0×10^{-5}
				(M_Z rec.$\rightarrow$)	0.13	1.4×10^{-4}
				(M_W rec.$\rightarrow$)	0.1	1.6×10^{-4}

TABLE V: Production cross sections (in fb) at the LHC for $pp \to H^{\pm\pm}H^{\mp} \to W^{\pm}W^{\pm}W^{\mp}H_1/W^{\pm}W^{\pm}W^{\mp}Z^0 \to JJ + \ell^{\pm}\ell^{\pm} + \not{E}_T$ and $pp \to H^{++}H^{--} \to W^+W^+W^-W^- \to JJ + \ell^{\pm}\ell^{\pm} + \not{E}_T$, and for the leading backgrounds. We take $M_{H^{\pm\pm}} = M_{H^{\pm}} = 600$ GeV for illustration. The rates after imposing each selection criterion, as described in the text, are shown.

The cross section for jjW^+W^+ is below $\mathcal{O}(10$ fb) after some basic acceptance cuts. The large jet mass cut will further reduce them. The results of the signal and backgrounds are summarized in Table V for $M_{H^{\pm\pm}} = M_{H^{\pm}} = 600$ GeV. We see once again that the cuts are very efficient in retaining the signal and the background can be suppressed to a negligible level. The difficulty is the rather small signal rate to begin with, at the order of 5×10^{-2} fb.

VII. DISCUSSIONS AND CONCLUSIONS

A. Discussion on Testing the Type II Seesaw Mechanism

We have discussed the general properties of the Type II seesaw mechanism for neutrino masses where the Higgs sector of the Standard Model is extended by adding an $SU(2)_L$ Higgs triplet, $\Delta \sim (1,3,1)$. As is well-known, in this scenario the neutrino mass matrix is given by $M_\nu = \sqrt{2}\, Y_\nu\, v_\Delta$, where v_Δ is the vacuum expectation value (vev) of the neutral component of the triplet and Y_ν is the Yukawa coupling. Once the electroweak symmetry is broken $v_\Delta = \mu\, v_0^2/\sqrt{2}\, M_\Delta^2$, where the dimension parameter μ defines the doublet-triplet mixing and M_Δ is the mass of the triplet. In the standard "high-scale" seesaw mechanism assuming $Y_\nu \approx 1$ and $\mu \sim M_\Delta \approx 10^{14-15}$ GeV one obtains the natural value for neutrino masses $m_\nu \approx 1$ eV. However, even if it is a natural scenario in this case one cannot hope to realize the direct test of the mechanism at future colliders. In this work we have focused on the possibility to observe at the LHC the fields responsible for the Type II seesaw mechanism. In this case assuming $M_\Delta \lesssim 1$ TeV one finds that

$Y_\nu \times \mu \lesssim 1.7 \times 10^{-8}$ GeV. Therefore, if one assumes $Y_\nu \approx 1$, $\mu \approx 10^{-8}$ GeV and one can think about the μ term as a soft-breaking term of the global $U(1)_L$ (or $U(1)_{B-L}$) symmetry. Since this possibility is appealing and there is hope to test the mechanism at the LHC we have laid out the general properties of the Higgs bosons for both their leptonic decays and gauge boson modes. We have also explored the sensitivity to search for those signals at the LHC. We now outline our general proposal in order to convincingly test the Type II seesaw mechanism.

We need the following necessary steps. First, the theory must account for the experimentally measured values of light neutrino masses and mixing angles, and then predict the physical couplings of the doubly and singly charged Higgs bosons. This was accomplished in Sec. III.

We need to establish the existence of the charged Higgs bosons and further confirm the Higgs triplet nature. This can be accomplished by observing the associated production of the singly and doubly charged Higgs bosons $H^{\pm\pm}H^{\mp}$. We wish to utilize the physics reach at the LHC for this purpose, so we limit ourself to the triplet mass in the range

$$110 \text{ GeV} \lesssim M_\Delta \lesssim 1 \text{ TeV}, \tag{62}$$

where the lower limit comes from the direct experimental bound, and the upper limit is roughly the LHC reach. With our minimal model assumption, the only other crucial parameter, the triplet vev v_Δ, determines the Higgs phenomenology. There are three typical regions which characterize the different searching strategies.

- $\underline{1 \text{ eV} \lesssim v_\Delta < 10^{-4} \text{ GeV}}$: In this case the leading decays of the charged Higgs bosons are $H^{++} \to e_i^+ e_j^+$ and $H^+ \to e_i^+ \bar{\nu}$. There are in total six lepton number violating channels for the doubly charged Higgs, and three channels for the singly charged Higgs. We thus expect to test the theory once we discover the doubly and singly charged Higgs bosons and determine their branching fractions of different flavor combinations, in accordance with the model predictions in the Type II seesaw scheme as presented in Table III.

- $\underline{v_\Delta \approx 10^{-4} \text{ GeV}}$: In this situation, $H^{++} \to e_i^+ e_j^+$ and $H^{++} \to W^+ W^+$, as well as $H^+ \to e_i^+ \bar{\nu}$ and $H^+ \to W^+ H_1$, $W^+ Z$, $t\bar{b}$ are all comparable. One may thus wish to observe not only the clean dilepton signals of lepton number violation, but also the gauge boson pairs or $t\bar{b}$. The simultaneous observation of both channels will give a direct measurement for v_Δ.

- $\underline{10^{-4} \text{ GeV} < v_\Delta \lesssim 1 \text{ GeV}}$: In this case the lepton number violating Higgs decays are suppressed. One then must confirm its mixing with SM doublets. Through the decays of $H^+ \to t\bar{b}$ and $H^+ \to$
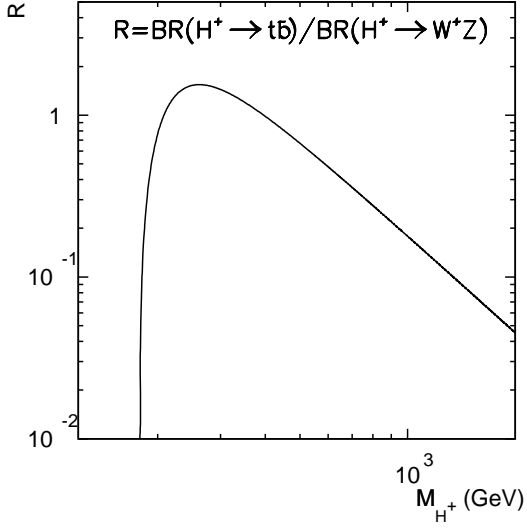
FIG. 32: Ratio between $BR(H^+ \to t\bar{b})$ and $BR(H^+ \to W^+Z)$ versus M^{H^+}.

W^+H_1, one can extract the μ parameter which defines the key relation for seesaw scheme $v_\Delta = \mu v_0^2/\sqrt{2}M_\Delta^2$ since

$$\Gamma(H^+ \to W^+H_1) \sim \frac{\mu^2}{M_{H^+}}, \quad \Gamma(H^+ \to t\bar{b}) \sim \frac{\mu^2 m_t^2}{M_{H^+}^3}, \tag{63}$$

and

$$\Gamma(H^+ \to W^+Z) \sim \left(g_1^2 \frac{\mu\, v_0^2}{M_\Delta^2} - \sqrt{2}(2g_1^2 + g_2^2)\, v_\Delta \right)^2 \frac{M_{H^+}^3}{v_0^4}. \tag{64}$$

In Fig. 32 the ratio between $BR(H^+ \to t\bar{b})$ and $BR(H^+ \to W^+Z)$ is shown which can be predicted once one uses the seesaw relation. The decay $H^+ \to t\bar{b}$ is dominant at low mass, and $H^+ \to W^+Z$ takes over for a heavier mass. Both channels should be searched for and they are complementary.

B. Conclusions

The possibility to test one of the most appealing mechanisms for neutrino mass generation, the so-called Type II seesaw mechanism, at the Large Hadron Collider has been investigated. We first emphasize the importance to observe the associated production $H^{\pm\pm}H^\mp$ to establish the gauge triplet nature of the Higgs field. We have found very encouraging results for further testing the theory.

In the optimistic scenarios, $1 \text{ eV} \lesssim v_\Delta < 10^{-4}$ GeV, one can test this theory to a great detail by looking for the clear signals of lepton number violation in the decays of doubly and singly charged Higgs bosons, at the LHC up to a mass about 1 TeV.

- Observing the difference in rate by comparing the decay channels for $H^{++} \to \mu^+\mu^+$, $\mu^+\tau^+$, $\tau^+\tau^+$ and $H^{++} \to e^+e^+$, $\mu^+\tau^+$, one could distinguish between the Normal Hierarchy and Inverted Hierarchy for the light neutrino mass spectrum, when the effect of the Majorana phases is not appreciable.

- If the Majorana phases play an important role, then the decay channels of H^{++} are less predicable. However, it is still possible to distinguish the neutrino spectrum by using the singly charged Higgs decay $H^+ \to e_i^+ \bar{\nu}$ $(e_i = e, \mu, \tau)$, which are independent of the Majorana phases. For a special case in IH, the significant changes in decay rate for the doubly charged Higgs $e^+e^+, \mu^+\tau^+ \leftrightarrow e^+\mu^+, e^+\tau^+$ will probe the phase Φ_1.

In the least favorable region of the parameter space, $v_\Delta > 10^{-4}$ GeV, where the lepton number violating processes are suppressed, we need to study the decays to SM gauge boson pairs or heavy quarks. Using the decays $H^+ \to t\bar{b}$ and $H^+ \to W^+H_1$ one could extract the μ parameter which defines the mixing between the SM Higgs doublet and the triplet, which in turn implies the existence of the same gauge interaction between the lepton doublet and the Higgs triplet. Therefore, we can check the seesaw relation $v_\Delta = \mu v_0^2/\sqrt{2}M_\Delta^2$ and the prediction for $H^+ \to W^+Z$.

In the most optimistic situation, $v_\Delta \sim 10^{-4}$ GeV, both channels of the lepton pairs and gauge boson pairs may be available simultaneously. The determination of their relative branching fractions would give a measurement for the value of v_Δ.

APPENDIX A: TYPE II SEESAW AND FEYNMANN RULES

As we have discussed in the previous sections the Type II seesaw mechanism [4] is one of the most appealing scenarios for the generation of neutrino masses. In this appendix we discuss in detail this

mechanism. In this extension of the Standard Model the Higgs sector is composed of the SM Higgs, $H \sim (1, 2, 1/2)$, and a complex triplet, $\Delta \sim (1, 3, 1)$:

$$H = \begin{pmatrix} \phi^+ \\ \phi^0 \end{pmatrix}, \quad \text{and} \quad \Delta = \begin{pmatrix} \delta^+/\sqrt{2} & \delta^{++} \\ \delta^0 & -\delta^+/\sqrt{2} \end{pmatrix} \tag{65}$$

The kinetic terms and relevant interactions in this theory are given in Eq. (2) and the new interactions for the leptons read as

$$\begin{aligned} \mathcal{L}_Y &= -Y_\nu \, l_L^T \, C \, i\sigma_2 \, \Delta \, l_L \, + \, h.c. \\ &= -Y_\nu \, \nu_L^T \, C \, \delta^0 \, \nu_L \, + \, \sqrt{2} \, Y_\nu \, \nu_L^T \, C \, \delta^+ \, e_L \, + \, Y_\nu \, e_L^T \, C \, \delta^{++} \, e_L \, + \, \text{h.c.} \end{aligned} \tag{66}$$

The scalar potential for H and Δ is given in Eq. (4). The simultaneous presence of the Yukawa coupling in Eq. (66) and the trilinear term proportional to the μ parameter in Eq. (4) tell us that the lepton number or $U(1)_L$ is explicitly broken.

Imposing the conditions of global minimum one finds that

$$-m_H^2 \, + \, \frac{\lambda}{4} v_0^2 \, - \, \sqrt{2} \, \mu \, v_\Delta = 0, \quad v_\Delta = \frac{\mu \, v_0^2}{\sqrt{2} \, M_\Delta^2}, \quad \text{and} \quad \lambda M_\Delta^2 - 4\mu^2 > 0, \tag{67}$$

where v_0 and v_Δ are the vacuum expectation values (vev) of the Higgs doublet and triplet, respectively, with $v_0^2 + v_\Delta^2 \approx (246 \text{ GeV})^2$. Once the neutral component in Δ gets the vev, $\langle \delta^0 \rangle = v_\Delta/\sqrt{2}$, the neutrino mass matrix is given by $M_\nu = \sqrt{2} \, Y_\nu \, v_\Delta$.

Higgs boson spectrum and gauge interactions

Let us compute the spectrum of the different Higgses present in the theory. Using

$$\phi^0 = (v_0 \, + \, h^0 \, + \, i\xi^0)/\sqrt{2}, \quad \text{and} \quad \delta^0 = (v_\Delta \, + \, \Delta^0 \, + \, i\eta^0)/\sqrt{2} \tag{68}$$

one finds that the mass matrix and the mixing angle for the CP-even states read as

$$\mathcal{M}_{\text{even}}^2 = \begin{pmatrix} \lambda \, v_0^2/2 & -\sqrt{2} \, \mu \, v_0 \\ -\sqrt{2} \, \mu \, v_0 & M_\Delta^2 \end{pmatrix} \quad \text{and} \quad \tan 2\theta_0 = -\frac{4 \, M_\Delta^2 \, v_\Delta}{v_0 \left(M_{H_1}^2 \, + \, M_{H_2}^2 \, - \, 2M_\Delta^2 \right)}, \tag{69}$$

$$H_1 = \cos \theta_0 \, h^0 \, + \, \sin \theta_0 \, \Delta^0, \quad H_2 = -\sin \theta_0 \, h^0 \, + \, \cos \theta_0 \, \Delta^0. \tag{70}$$

where $\sqrt{v_0^2 + v_\Delta^2} \approx 246$ GeV. The mass matrix and the mixing angle for the CP-odd states are given by:

$$\mathcal{M}_{\text{odd}}^2 = \begin{pmatrix} 2\sqrt{2} \, \mu \, v_\Delta & -\sqrt{2} \, \mu \, v_0 \\ -\sqrt{2} \, \mu \, v_0 & M_\Delta^2 \end{pmatrix} \quad \text{and} \quad \tan 2\alpha = -\frac{4 \, M_\Delta^2 \, v_\Delta}{v_0 \left(M_A^2 - 2M_\Delta^2 \right)}, \tag{71}$$

$$G = \cos \alpha \, \xi^0 \, + \, \sin \alpha \, \eta^0, \quad A = -\sin \alpha \, \xi^0 \, + \, \cos \alpha \, \eta^0. \tag{72}$$

Vertices	Gauge Couplings	Approximation
$H^{++}H^-W_\mu^-$	$-ig_2\cos\theta_+(p_1-p_2)_\mu$	$-ig_2(p_1-p_2)_\mu$
$H^{++}W_\mu^-W_\nu^-$	$i\sqrt{2}g_2^2 v_\Delta g_{\mu\nu}$	$i\sqrt{2}g_2^2 v_\Delta g_{\mu\nu}$
$H^+H_2W_\mu^-$	$-i\frac{g_2}{2}(\sqrt{2}\cos\theta_+\cos\theta_0+\sin\theta_0\sin\theta_+)(p_1-p_2)_\mu$	$-i\frac{g_2}{\sqrt{2}}(p_1-p_2)_\mu$
$H^+AW_\mu^-$	$\frac{g_2}{2}(\sqrt{2}\cos\theta_+\cos\alpha+\sin\alpha\sin\theta_+)(p_1-p_2)_\mu$	$\frac{g_2}{\sqrt{2}}(p_1-p_2)_\mu$
$H^+H_1W_\mu^-$	$-i\frac{g_2}{2}(\sqrt{2}\cos\theta_+\sin\theta_0-\cos\theta_0\sin\theta_+)(p_1-p_2)_\mu$	$-i\frac{g_2}{2}\frac{\mu v_0}{M_\Delta^2}(p_1-p_2)_\mu$
$H^+Z_\mu W_\nu^-$	$i\frac{\cos\theta_W}{2}(g_1^2\sin\theta_+v_0-\sqrt{2}\cos\theta_+(2g_1^2+g_2^2)v_\Delta)g_{\mu\nu}$	$i\frac{g_2^2\sin^2\theta_W}{2\cos\theta_W}(\frac{\mu v_0^2}{M_\Delta^2}-\sqrt{2}(2+\cot^2\theta_W)v_\Delta)g_{\mu\nu}$
$H_2H_1H_1$	$i\frac{1}{4}\cos\theta_0(3\sin2\theta_0\lambda v_0+4\sqrt{2}\cos2\theta_0\mu-4\sqrt{2}\sin^2\theta_0\mu)$	$i(\sqrt{2}\mu+\frac{3}{2}\lambda\frac{\sqrt{2}\mu v_0^2}{M_\Delta^2})$
$H_2W_\mu^+W_\nu^-$	$-i\frac{1}{2}g_2^2(\sin\theta_0 v_0-2\cos\theta_0 v_\Delta)g_{\mu\nu}$	$-i\frac{1}{2}g_2^2(\frac{\sqrt{2}\mu v_0^2}{M_\Delta^2}-2v_\Delta)g_{\mu\nu}$
$H_2Z_\mu Z_\nu$	$-i\frac{1}{2}\frac{g_2^2}{\cos^2\theta_W}(\sin\theta_0 v_0-4\cos\theta_0 v_\Delta)g_{\mu\nu}$	$-i\frac{1}{2}\frac{g_2^2}{\cos^2\theta_W}(\frac{\sqrt{2}\mu v_0^2}{M_\Delta^2}-4v_\Delta)g_{\mu\nu}$
AH_1Z_μ	$\frac{g_2}{2\cos\theta_W}(\cos\theta_0\sin\alpha-2\cos\alpha\sin\theta_0)(p_1-p_2)_\mu$	$-\frac{g_2}{\sqrt{2}\cos\theta_W}\frac{\mu v_0}{M_\Delta^2}(p_1-p_2)_\mu$

TABLE VI: Feynman rules for the heavy Higgs boson gauge Interactions. The momenta are all assumed to be incoming, and p_1 (p_2) refers to the first (second) scalar field listed in the vertices. The approximation is based on $v_0 \gg v_\Delta$, $M_\Delta > M_{H_1}$.

In the singly charged Higgs sector (ϕ^+, δ^+), the mass matrix and the mixing angle for the physical states read as

$$\mathcal{M}_\pm^2 = \begin{pmatrix} \sqrt{2}\mu\, v_\Delta & -\mu\, v_0 \\ -\mu\, v_0 & M_\Delta^2 \end{pmatrix} \quad \text{and} \quad \tan 2\theta_+ = -\frac{2\sqrt{2}\, v_\Delta\, M_\Delta^2}{v_0\left(M_{H^+}^2-2M_\Delta^2\right)}, \tag{73}$$

$$G^\pm = \cos\theta_\pm\,\phi^\pm + \sin\theta^\pm\,\delta^\pm, \quad H^\pm = -\sin\theta_\pm\,\phi^\pm + \cos\theta_\pm\,\delta^\pm. \tag{74}$$

There are thus seven physical mass eigenstates: H_1 (SM-Like), H_2 (Δ-Like), A, $H^\pm$, and $H^{\pm\pm} = \delta^{\pm\pm}$. In this minimal setting,

$$M_{H_2} \simeq M_A \simeq M_{H^\pm} \simeq M_{H^{\pm\pm}} = M_\Delta. \tag{75}$$

The mixing angles in all sectors are very small since $v_\Delta \ll v_0$. It is thus useful to write down the approximations

$$\tan 2\theta_0 \approx \frac{-2\sqrt{2}\mu v_0}{M_{H_1}^2-M_\Delta^2} \approx 4\frac{v_\Delta}{v_0}, \quad \tan 2\alpha \approx \frac{2\sqrt{2}\mu v_0}{M_\Delta^2} = 4\frac{v_\Delta}{v_0}, \quad \tan 2\theta_+ \approx \frac{2\mu v_0}{M_\Delta^2} = 2\sqrt{2}\frac{v_\Delta}{v_0}. \tag{76}$$

The Feynmann rules for the Higgs boson gauge interactions are listed in Table VI.

Heavy Higgs boson Yukawa interactions via mixing

The triplet fields mix with the Higgs doublet via the dimensional parameter μ. Thus the Standard Model Yukawa interactions will yield the heavy Higgs couplings to the SM fermions. The Feynman rules are listed

Vertices	Yukawa Couplings	Approximation
$H^+ \bar{t} b$	$-i\sqrt{2}\frac{m_t P_L + m_b P_R}{v_0}\sin\theta_+$	$-i\sqrt{2}\frac{m_t \mu}{M_\Delta^2}P_L$
$H_2 f \bar{f}$	$-i\frac{m_f}{v_0}\sin\theta_0$	$-i\sqrt{2}\frac{m_f \mu}{M_\Delta^2}P_L$
$A f \bar{f}$	$\gamma_5 \frac{m_f}{v_0}\sin\alpha$	$\sqrt{2}\gamma_5 \frac{m_f \mu}{M_\Delta^2}$

TABLE VII: Feynman rules for the heavy Higgs boson Yukawa Interactions via mixing μ.

Fields	Vertices	Yukawa Couplings	Approximation
H^{++}	$H^{++}e_i^{-T}e_j^-$	$C2\Gamma_{++}^{ij}P_L$	$C2\Gamma_{++}^{ij}P_L$
H^+	$H^+\nu_i^T e_j^-$	$C\Gamma_+^{ij}P_L$	$C\Gamma_+^{ij}P_L$
H_2	$H_2\nu_i^T\nu_i\ (\bar{\nu}_i\bar{\nu}_i)$	$C\cos\theta_0\ (m_{\nu_i}/v_\Delta)\ P_L$	$C(m_{\nu_i}/v_\Delta)\ P_L$
A	$A\nu_i^T\nu_i\ (\bar{\nu}_i\bar{\nu}_i)$	$C\cos\alpha\ (m_{\nu_i}/v_\Delta)\ P_L$	$C(m_{\nu_i}/v_\Delta)\ P_L$

TABLE VIII: Yukawa Interactions for lepton number violating vertices.

in Table VII.

Heavy Higgs boson $\Delta L = 2$ Yukawa interactions

The physical interactions in the Yukawa sector are given in Eq. (11) and Eq. (12). We present the Yukawa couplings for lepton number violating vertices in Table VIII.

The explicit couplings in terms of the neutrino mass and mixing parameters are as follows:

$$\Gamma_+ = \cos\theta_+ \frac{m_\nu^{diag} V_{PMNS}^\dagger}{v_\Delta}, \quad \text{and} \quad \Gamma_{++} = \frac{V_{PMNS}^* m_\nu^{diag} V_{PMNS}^\dagger}{\sqrt{2}\, v_\Delta} \equiv Y_\nu, \tag{77}$$

and in the text we have defined squared sum relevant for the singly charged Higgs processes

$$Y_+^j = \sum_{i=1}^3 |\Gamma_+^{ij}|^2 \times v_\Delta^2, \tag{78}$$

where

$$
\begin{aligned}
Y_+^1 &= m_1^2 c_{12}^2 c_{13}^2 + m_2^2 c_{13}^2 s_{12}^2 + m_3^2 s_{13}^2 \\
Y_+^2 &= \left(c_{23}^2 m_2^2 + m_1^2 s_{13}^2 s_{23}^2\right) c_{12}^2 + 2\cos(\delta)c_{23}\left(m_1^2 - m_2^2\right)s_{12}s_{13}s_{23}c_{12} \\
&\quad + c_{23}^2 m_1^2 s_{12}^2 + \left(c_{13}^2 m_3^2 + m_2^2 s_{12}^2 s_{13}^2\right)s_{23}^2 \\
Y_+^3 &= \left(c_{23}^2 m_1^2 s_{13}^2 + m_2^2 s_{23}^2\right)c_{12}^2 - 2\cos(\delta)c_{23}\left(m_1^2 - m_2^2\right)s_{12}s_{13}s_{23}c_{12} \\
&\quad + c_{13}^2 c_{23}^2 m_3^2 + s_{12}^2\left(c_{23}^2 m_2^2 s_{13}^2 + m_1^2 s_{23}^2\right)
\end{aligned}
$$

$$\sqrt{2}v_\Delta\Gamma_{++}^{11} = m_1 e^{-i\Phi_1} c_{12}^2 c_{13}^2 + m_2 s_{12}^2 c_{13}^2 + m_3 e^{i(2\delta-\Phi_2)} s_{13}^2$$

$$\sqrt{2}v_\Delta\Gamma_{++}^{22} = m_1 e^{-i\Phi_1}\left(-s_{12}c_{23} - e^{-i\delta}c_{12}s_{13}s_{23}\right)^2 + m_2\left(c_{12}c_{23} - e^{-i\delta}s_{12}s_{13}s_{23}\right)^2 + m_3 e^{-i\Phi_2}c_{13}^2 s_{23}^2$$

$$\sqrt{2}v_\Delta\Gamma_{++}^{33} = m_1 e^{-i\Phi_1}\left(s_{12}s_{23} - e^{-i\delta}c_{12}s_{13}c_{23}\right)^2 + m_2\left(-c_{12}s_{23} - e^{-i\delta}s_{12}s_{13}c_{23}\right)^2 + m_3 e^{-i\Phi_2}c_{13}^2 c_{23}^2$$

$$\sqrt{2}v_\Delta\Gamma_{++}^{12} = m_1 e^{-i\Phi_1}c_{12}c_{13}\left(-s_{12}c_{23} - e^{-i\delta}c_{12}s_{13}s_{23}\right) + m_2 s_{12}c_{13}\left(c_{12}c_{23} - e^{-i\delta}s_{12}s_{13}s_{23}\right)$$
$$+ \; m_3 e^{i(\delta-\Phi_2)}s_{13}c_{13}s_{23}$$

$$\sqrt{2}v_\Delta\Gamma_{++}^{13} = m_1 e^{-i\Phi_1}c_{12}c_{13}\left(s_{12}s_{23} - e^{-i\delta}c_{12}c_{23}s_{13}\right) + m_2 c_{13}s_{12}\left(-c_{12}s_{23} - e^{-i\delta}s_{12}s_{13}c_{23}\right)$$
$$+ \; m_3 e^{i(\delta-\Phi_2)}s_{13}c_{13}c_{23}$$

$$\sqrt{2}v_\Delta\Gamma_{++}^{23} = m_1 e^{-i\Phi_1}\left(s_{12}s_{23} - e^{-i\delta}c_{12}s_{13}c_{23}\right)\left(-s_{12}c_{23} - e^{-i\delta}c_{12}s_{13}s_{23}\right)$$
$$+ \; m_2\left(-c_{12}s_{23} - e^{-i\delta}s_{12}s_{13}c_{23}\right)\left(c_{12}c_{23} - e^{-i\delta}s_{12}s_{13}s_{23}\right) + m_3 e^{-i\Phi_2}c_{13}^2 s_{23}c_{23}$$

APPENDIX B: DECAYS OF H^{++}, H^+, H_2 AND A

The expressions for the relevant partial decay widths are the following:

Doubly Charged Higgs:

$$\Gamma(H^{++} \to e_i^+ e_j^+) = \frac{1}{4\pi(1+\delta_{ij})}|\Gamma_{++}^{ij}|^2 M_{H^{++}} \tag{79}$$

$$\Gamma(H^{++} \to W_T^+ W_T^+) = \frac{g_2^4 v_\Delta^2}{8\pi M_{H^{++}}}\lambda^{\frac{1}{2}}(1, r_W^2, r_W^2) \approx \frac{g_2^2 M_W^2 v_\Delta^2}{2\pi M_{H^{++}}v_0^2} \tag{80}$$

$$\Gamma(H^{++} \to W_L^+ W_L^+) = \frac{g_2^4 v_\Delta^2}{16\pi M_{H^{++}}}\lambda^{\frac{1}{2}}(1, r_W^2, r_W^2)\frac{(1-2r_W^2)^2}{4r_W^4} \approx \frac{M_{H^{++}}^3 v_\Delta^2}{4\pi v_0^4} \tag{81}$$

$$\Gamma(H^{++} \to H^+\pi^+) = \frac{g_2^4 V_{ud}^2 \Delta M^3 f_\pi^2}{16\pi M_W^4} \tag{82}$$

$$\Gamma(H^{++} \to H^+ e^+(\mu^+)\nu_e(\nu_\mu)) = \frac{g_2^4 \Delta M^5}{240\pi^3 M_W^4} \tag{83}$$

$$\Gamma(H^{++} \to H^+ q\bar{q}') = 3\Gamma(H^{++} \to H^+ e^+(\mu^+)\nu_e(\nu_\mu)) \tag{84}$$

where $\Delta M = M_{H++} - M_{H+}$ and $r_i = M_i/M_\Delta$.

Singly Charged Higgs:

$$\Gamma(H^+ \to \ell_i^+ \bar{\nu}_j) = \frac{1}{16\pi}|\Gamma_+^{ij}|^2 M_{H^+} \tag{85}$$

$$\Gamma(H^+ \to W_T^+ Z_T) = \frac{\cos^2\theta_W}{32\pi M_{H^+}}\left(g_1^2\sin\theta_+ \, v_0 \, - \, \sqrt{2}\cos\theta_+ \, (2g_1^2+g_2^2)\, v_\Delta\right)^2 \lambda^{\frac{1}{2}}(1, r_W^2, r_Z^2)$$

$$\approx \frac{g_2^2 \sin^4\theta_W M_Z^2}{8\pi M_{H^+}v_0^2}(\frac{\mu v_0^2}{M_{H^+}^2} - \sqrt{2}(2+\cot^2\theta_W)v_\Delta)^2 = \frac{g_2^2 M_Z^2 v_\Delta^2}{4\pi M_{H^+}v_0^2} \tag{86}$$

$$\Gamma(H^+ \to W_L^+ Z_L) = \frac{\cos^2\theta_W}{64\pi M_{H^+}}\left(g_1^2\sin\theta_+ \, v_0 \, - \, \sqrt{2}\cos\theta_+ \, (2g_1^2+g_2^2)\, v_\Delta\right)^2 \lambda^{\frac{1}{2}}(1, r_W^2, r_Z^2)\frac{(1-r_W^2-r_Z^2)^2}{4r_W^2 r_Z^2}$$

$$\approx \frac{M_{H^+}^3 \sin^4\theta_W}{16\pi v_0^4}(\frac{\mu v_0^2}{M_{H^+}^2} - \sqrt{2}(2+\cot^2\theta_W)v_\Delta)^2 = \frac{M_{H^+}^3 v_\Delta^2}{8\pi v_0^4} \tag{87}$$

$$\Gamma(H^+ \to W_L^+ H_1) = \frac{M_{H^+} g_2^2}{64\pi r_W^2}\left(\sqrt{2}\cos\theta_+ \, \sin\theta_0 \, - \, \sin\theta_+ \, \cos\theta_0\right)^2 \lambda^{\frac{3}{2}}(1, r_W^2, r_{H_1}^2)$$

$$\approx \frac{\mu^2}{16\pi M_{H^+}} = \frac{M_{H^+}^3 v_\Delta^2}{8\pi v_0^4} \tag{88}$$

$$\Gamma(H^+ \to t\bar{b}) = \frac{N_c M_{H^+} m_t^2 \sin^2\theta_+}{8\pi v_0^2}\lambda^{\frac{1}{2}}(1, r_t^2, r_b^2)(1-r_t^2-r_b^2) \approx \frac{N_c \mu^2 m_t^2}{8\pi M_{H^+}^3} = \frac{N_c M_{H^+} m_t^2 v_\Delta^2}{4\pi v_0^4} \tag{89}$$

Heavy CP-even Higgs:

$$\Gamma(H_2 \to \nu_i\nu_i + \bar{\nu}_i\bar{\nu}_i) = \frac{1}{16\pi}\cos^2\theta_0 \frac{m_{\nu_i}^2}{v_\Delta^2}M_{H_2} \approx \frac{m_{\nu_i}^2}{16\pi v_\Delta^2}M_{H_2} \tag{90}$$

$$\Gamma(H_2 \to Z_T Z_T) = \frac{g_2^4}{64\pi M_{H_2}\cos^4\theta_W}(\sin\theta_0 \, v_0 \, - \, 4\cos\theta_0 \, v_\Delta)^2 \lambda^{\frac{1}{2}}(1, r_Z^2, r_Z^2)$$

$$\approx \frac{g_2^2 m_Z^2}{16\pi M_{H_2}\cos^2\theta_W v_0^2}(\frac{\sqrt{2}\mu v_0^2}{M_{H_2}^2} - 4v_\Delta)^2 = \frac{g_2^2 m_Z^2 v_\Delta^2}{4\pi M_{H_2}\cos^2\theta_W v_0^2} \tag{91}$$

$$\Gamma(H_2 \to Z_L Z_L) = \frac{g_2^4}{128\pi M_{H_2}\cos^4\theta_W}(\sin\theta_0 \, v_0 \, - \, 4\cos\theta_0 \, v_\Delta)^2 \lambda^{\frac{1}{2}}(1, r_Z^2, r_Z^2)\frac{(1-2r_Z^2)^2}{4r_Z^4}$$

$$\approx \frac{M_{H_2}^3}{32\pi v_0^4}(\frac{\sqrt{2}\mu v_0^2}{M_{H_2}^2} - 4v_\Delta)^2 = \frac{M_{H_2}^3 v_\Delta^2}{8\pi v_0^4} \tag{92}$$

$$\Gamma(H_2 \to H_1 H_1) = \frac{1}{512\pi M_{H_2}}\cos\theta_0^2\left(3\sin2\theta_0\lambda v_0 \, + \, 4\sqrt{2}\cos2\theta_0 \, \mu \, - \, 4\sqrt{2}\sin^2\theta_0 \, \mu\right)^2 \lambda^{\frac{1}{2}}(1, r_{H_1}^2, r_{H_1}^2)$$

$$\approx \frac{1}{32\pi M_{H_2}}(\frac{6M_{H_1}^2 v_\Delta}{v_0^2} + \sqrt{2}\mu)^2 \approx \frac{\mu^2}{16\pi M_{H_2}} = \frac{M_{H_2}^3 v_\Delta^2}{8\pi v_0^4} \tag{93}$$

$$\Gamma(H_2 \to t\bar{t}) = \frac{N_c M_{H_2} m_t^2 \sin^2\theta_0}{8\pi v_0^2}\lambda^{\frac{1}{2}}(1, r_t^2, r_t^2)(1-4r_t^2) \approx \frac{N_c m_t^2 \mu^2}{4\pi M_{H_2}^3} = \frac{N_c M_{H_2} m_t^2 v_\Delta^2}{2\pi v_0^4} \tag{94}$$

$$\Gamma(H_2 \to b\bar{b}) = \frac{N_c M_{H_2} m_b^2 \sin^2\theta_0}{8\pi v_0^2}\lambda^{\frac{1}{2}}(1, r_b^2, r_b^2)(1-4r_b^2) \approx \frac{N_c m_b^2 \mu^2}{4\pi M_{H_2}^3} = \frac{N_c M_{H_2} m_b^2 v_\Delta^2}{2\pi v_0^4} \tag{95}$$

CP-odd Higgs:

$$\Gamma(A \to \nu_i \nu_i + \bar{\nu}_i \bar{\nu}_i) = \frac{1}{16\pi}\cos^2\alpha\frac{m_{\nu_i}^2}{v_\Delta^2}M_A \approx \frac{m_{\nu_i}^2}{16\pi v_\Delta^2}M_A \tag{96}$$

$$\Gamma(A \to Z_L H_1) = \frac{M_A g_2^2}{64\pi r_Z^2 \cos^2\theta_W}\left(\cos\theta_0\sin\alpha - 2\sin\theta_0\cos\alpha\right)^2 \lambda^{\frac{3}{2}}(1, r_{H_1}^2, r_Z^2)$$

$$\approx \frac{\mu^2}{8\pi M_A} = \frac{M_A^3 v_\Delta^2}{4\pi v_0^4} \tag{97}$$

$$\Gamma(A \to t\bar{t}) = \frac{N_c M_A m_t^2 \sin^2\alpha}{8\pi v_0^2}\lambda^{\frac{1}{2}}(1, r_t^2, r_t^2) \approx \frac{N_c \mu^2 m_t^2}{4\pi M_A^3} = \frac{N_c M_A m_t^2 v_\Delta^2}{2\pi v_0^4} \tag{98}$$

$$\Gamma(A \to b\bar{b}) = \frac{N_c M_A m_b^2 \sin^2\alpha}{8\pi v_0^2}\lambda^{\frac{1}{2}}(1, r_b^2, r_b^2) \approx \frac{N_c \mu^2 m_b^2}{4\pi M_A^3} = \frac{N_c M_A m_b^2 v_\Delta^2}{2\pi v_0^4} \tag{99}$$

[1] For recent reviews on neutrino physics, see *e.g.*, V. Barger, D. Marfatia, and K. Whisnant, Int. J. Mod. Phys. **E12**, 569 (2003); B. Kayser, p. 145 of the Review of Particle Physics, Phys. Lett. **B592**, 1 (2004); M. C. Gonzalez-Garcia and M. Maltoni, "Phenomenology with Massive Neutrinos," arXiv:0704.1800 [hep-ph]; R. N. Mohapatra and A. Y. Smirnov, "Neutrino mass and new physics," Ann. Rev. Nucl. Part. Sci. **56** (2006) 569 [arXiv:hep-ph/0603118]; A. Strumia and F. Vissani, "Neutrino masses and mixings and.," arXiv:hep-ph/0606054.

[2] S. Weinberg, "Baryon And Lepton Nonconserving Processes," Phys. Rev. Lett. **43** (1979) 1566.

[3] P. Minkowski, "$\mu \to e\gamma$ at a rate of one out of 1-Billion muon decays?," Phys. Lett. B **67** (1977) 421; T. Yanagida, in *Proceedings of the Workshop on the Unified Theory and the Baryon Number in the Universe*, eds. O. Sawada et al., (KEK Report 79-18, Tsukuba, 1979), p. 95; M. Gell-Mann, P. Ramond and R. Slansky, in *Supergravity*, eds. P. van Nieuwenhuizen et al., (North-Holland, 1979), p. 315; S.L. Glashow, in *Quarks and Leptons*, Cargèse, eds. M. Lévy et al., (Plenum, 1980), p. 707; R. N. Mohapatra and G. Senjanović, "Neutrino Mass And Spontaneous Parity Nonconservation," Phys. Rev. Lett. **44** (1980) 912.

[4] W. Konetschny and W. Kummer, "Nonconservation Of Total Lepton Number With Scalar Bosons," Phys. Lett. B **70** (1977) 433; T. P. Cheng and L. F. Li, "Neutrino Masses, Mixings And Oscillations In SU(2) X U(1) Models Of Electroweak Interactions," Phys. Rev. D **22** (1980) 2860; G. Lazarides, Q. Shafi and C. Wetterich, "Proton Lifetime And Fermion Masses In An SO(10) Model," Nucl. Phys. B **181** (1981) 287; J. Schechter and J. W. F. Valle, "Neutrino Masses In SU(2) X U(1) Theories," Phys. Rev. D **22** (1980) 2227; R. N. Mohapatra and G. Senjanović, "Neutrino Masses And Mixings In Gauge Models with Spontaneous Parity Violation," Phys. Rev. D **23** (1981) 165.

[5] R. Foot, H. Lew, X. G. He and G. C. Joshi, "seesaw neutrino masses induced by a triplet of leptons," Z. Phys. C **44** (1989) 441.

[6] E. Ma, "Pathways to naturally small neutrino masses," Phys. Rev. Lett. **81** (1998) 1171 [arXiv:hep-ph/9805219]; B. Bajc and G. Senjanović, "seesaw at LHC," JHEP **0708** (2007) 014 [arXiv:hep-ph/0612029]; P. Fileviez Pérez, "Renormalizable Adjoint SU(5)," Phys. Lett. B **654** (2007) 189 [arXiv:hep-ph/0702287]; P. Fileviez Pérez, "Supersymmetric Adjoint SU(5)," Phys. Rev. D **76** (2007) 071701 [arXiv:0705.3589 [hep-ph]].

[7] R. N. Mohapatra and J. C. Pati, "A Natural Left-Right Symmetry," Phys. Rev. D **11** (1975) 2558; G. Senjanović and R. N. Mohapatra, "Exact Left-Right Symmetry And Spontaneous Violation Of Parity," Phys. Rev. D **12** (1975) 1502; G. Senjanović, "Spontaneous Breakdown Of Parity In A Class Of Gauge Theories," Nucl. Phys. B **153** (1979) 334.

[8] A. Zee, "A Theory Of Lepton Number Violation, Neutrino Majorana Mass, And Oscillation," Phys. Lett. B **93** (1980) 389 [Erratum-ibid. B **95** (1980) 461]; K. S. Babu, "Model of 'Calculable' Majorana Neutrino Masses," Phys. Lett. B **203** (1988) 132; K. S. Babu and C. Macesanu, "Two-loop neutrino mass generation and its experimental consequences," Phys. Rev. D **67** (2003) 073010 [arXiv:hep-ph/0212058].

[9] A. de Gouvea, J. Jenkins and N. Vasudevan, "Neutrino phenomenology of very low-energy seesaws," Phys. Rev. D **75**, 013003 (2007) [arXiv:hep-ph/0608147]; A. de Gouvea, "GeV seesaw, Accidentally Small Neutrino Masses, and Higgs Decays to Neutrinos," arXiv:0706.1732 [hep-ph].

[10] I. Dorsner and P. Fileviez Pérez, "Unification without supersymmetry: Neutrino mass, proton decay and light leptoquarks," Nucl. Phys. B **723** (2005) 53 [arXiv:hep-ph/0504276]. See also: I. Dorsner, P. Fileviez Pérez and R. Gonzalez Felipe, "Phenomenological and cosmological aspects of a minimal GUT scenario," Nucl. Phys. B **747** (2006) 312 [arXiv:hep-ph/0512068]; P. Fileviez Pérez, "Upper bound on the proton lifetime and the minimal non-SUSY grand unified theory," AIP Conf. Proc. **903** (2006) 385 [arXiv:hep-ph/0606279]; I. Dorsner, P. Fileviez Pérez and G. Rodrigo, "Fermion Masses and the UV Cutoff of the Minimal Realistic SU(5)," Phys. Rev. D **75** (2007) 125007 [arXiv:hep-ph/0607208]; I. Dorsner and P. Fileviez Pérez, "Unification versus proton decay in SU(5)," Phys. Lett. B **642** (2006) 248 [arXiv:hep-ph/0606062].

[11] I. Dorsner and P. Fileviez Perez, "Upper Bound on the Mass of the Type III Seesaw Triplet in an SU(5) Model," JHEP **0706**, 029 (2007) [arXiv:hep-ph/0612216]; B. Bajc, M. Nemevsek and G. Senjanović, "Probing seesaw at LHC," Phys. Rev. D **76**, 055011 (2007) [arXiv:hep-ph/0703080]; E. Ma and D. P. Roy, "Heavy triplet leptons and new gauge boson," Nucl. Phys. B **644** (2002) 290 [arXiv:hep-ph/0206150].

[12] W. Y. Keung and G. Senjanović, "Majorana Neutrinos And The Production Of The Right-Handed Charged Gauge Boson," Phys. Rev. Lett. **50** (1983) 1427; D. A. Dicus, D. D. Karatas and P. Roy, "Lepton nonconservation at supercollider energies," Phys. Rev. D **44** (1991) 2033; A. Datta, M. Guchait and A. Pilaftsis, "Probing lepton number violation via majorana neutrinos at hadron supercolliders," Phys. Rev. D **50** (1994) 3195; F. M. L. Almeida, Y. D. A. Coutinho, J. A. Martins Simoes and M. A. B. do Vale, "On a signature for heavy Majorana neutrinos in hadronic collisions," Phys. Rev. D **62** (2000) 075004; O. Panella, M. Cannoni, C. Carimalo and Y. N. Srivastava, "Signals of heavy Majorana neutrinos at hadron colliders," Phys. Rev. D **65** (2002) 035005.

[13] T. Han and B. Zhang, "Signatures for Majorana neutrinos at hadron colliders," Phys. Rev. Lett. **97**, 171804 (2006).

[14] For a comparison for different colliders, see *e.g.*, F. del Aguila, J. A. Aguilar-Saavedra and R. Pittau, "Neutrino physics at large colliders," J. Phys. Conf. Ser. **53**, 506 (2006) [arXiv:hep-ph/0606198]; F. del Aguila, J. A. Aguilar-Saavedra and R. Pittau, "Heavy neutrino signals at large hadron colliders," JHEP **0710**, 047 (2007) [arXiv:hep-ph/0703261]; J. Kersten and A. Y. Smirnov, "Right-Handed Neutrinos at LHC and the Mechanism

of Neutrino Mass Generation," Phys. Rev. D **76**, 073005 (2007) [arXiv:0705.3221 [hep-ph]]; S. Bar-Shalom, G. Eilam, T. Han and A. Soni, "Charged Higgs Boson Effects in the Production and Decay of a Heavy Majorana Neutrino at the LHC," arXiv:0803.2835 [hep-ph].

[15] R. Franceschini, T. Hambye and A. Strumia, arXiv:0805.1613 [hep-ph].

[16] E. J. Chun, K. Y. Lee and S. C. Park, "Testing Higgs triplet model and neutrino mass patterns," Phys. Lett. B **566** (2003) 142 [arXiv:hep-ph/0304069]; T. Han, H. E. Logan, B. Mukhopadhyaya and R. Srikanth, "Neutrino masses and lepton-number violation in the littlest Higgs scenario," Phys. Rev. D **72**, 053007 (2005) [arXiv:hep-ph/0505260]; C. S. Chen, C. Q. Geng, J. N. Ng and J. M. S. Wu, "Testing Radiative Neutrino Mass Generation at the LHC," JHEP **0708** (2007) 022 [arXiv:0706.1964 [hep-ph]].

[17] A. Hektor, M. Kadastik, M. Muntel, M. Raidal and L. Rebane, "Testing neutrino masses in little Higgs models via discovery of doubly charged Higgs at LHC," Nucl. Phys. B **787**, 198 (2007) [arXiv:0705.1495 [hep-ph]].

[18] T. Han, B. Mukhopadhyaya, Z. Si and K. Wang, "Pair Production of Doubly-Charged Scalars: Neutrino Mass Constraints and Signals at the LHC," Phys. Rev. D **76**, 075013 (2007) [arXiv:0706.0441 [hep-ph]].

[19] J. Garayoa and T. Schwetz, "Neutrino mass hierarchy and Majorana CP phases within the Higgs triplet model at the LHC," arXiv:0712.1453 [hep-ph].

[20] M. Kadastik, M. Raidal and L. Rebane, "Direct determination of neutrino mass parameters at future colliders," arXiv:0712.3912 [hep-ph].

[21] A. G. Akeroyd, M. Aoki and H. Sugiyama, "Probing Majorana Phases and Neutrino Mass Spectrum in the Higgs Triplet Model at the LHC," arXiv:0712.4019 [hep-ph].

[22] W. Chao, S. Luo, Z. Z. Xing and S. Zhou, "A Compromise between Neutrino Masses and Collider Signatures in the Type-II Seesaw Model," Phys. Rev. D **77**, 016001 (2008) [arXiv:0709.1069 [hep-ph]]; W. Chao, Z. G. Si, Z. Z. Xing and S. Zhou, "Correlative signatures of heavy Majorana neutrinos and doubly-charged Higgs arXiv:0804.1265 [hep-ph].

[23] P. Fileviez Pérez, T. Han, G. Y. Huang, T. Li and K. Wang, "Testing a Neutrino Mass Generation mechanism at the LHC," arXiv:0803.3450 [hep-ph].

[24] T. Schwetz, "Neutrino oscillations: present status and outlook," arXiv:0710.5027 [hep-ph]; M. Maltoni, T. Schwetz, M. A. Tortola and J. W. F. Valle, "Status of global fits to neutrino oscillations," New J. Phys. **6** (2004) 122 [arXiv:hep-ph/0405172].

[25] A. Abada, C. Biggio, F. Bonnet, M. B. Gavela and T. Hambye, "Low energy effects of neutrino masses," arXiv:0707.4058 [hep-ph].

[26] W. M. Yao *et al.* [Particle Data Group], "Review of particle physics," J. Phys. G **33** (2006) 1.

[27] V. M. Abazov *et al.* [D0 Collaboration], "Search for doubly-charged Higgs boson pair production in the decay to $\mu^+\mu^+\mu^-\mu^-$ in $p\bar{p}$ collisions at $\sqrt{s} = 1.96$ TeV," Phys. Rev. Lett. **93** (2004) 141801 [arXiv:hep-ex/0404015]; D. E. Acosta *et al.* [CDF Collaboration], "Search for doubly-charged Higgs bosons decaying to dileptons in $p\bar{p}$ collisions at $\sqrt{s} = 1.96$ TeV," Phys. Rev. Lett. **93** (2004) 221802 [arXiv:hep-ex/0406073]; V. M. Abazov *et al.* [D0 Collaboration], arXiv:0803.1534 [hep-ex] .

[28] J. F. Gunion, R. Vega and J. Wudka, "Naturalness Problems For Rho = 1 And Other Large One Loop Effects For

A Standard Model Higgs Sector Containing Triplet Fields," Phys. Rev. D **43** (1991) 2322.

[29] M. Cirelli, N. Fornengo and A. Strumia, "Minimal dark matter," Nucl. Phys. B **753** (2006) 178 [arXiv:hep-ph/0512090].

[30] See *e. g.*, D. Autiero *et al.*, "Large underground, liquid based detectors for astro-particle physics in Europe: scientific case and prospects," JCAP **0711** (2007) 011 [arXiv:0705.0116 [hep-ph]].

[31] A. G. Akeroyd and M. Aoki, "Single and pair production of doubly charged Higgs bosons at hadron colliders," Phys. Rev. D **72**, 035011 (2005) [arXiv:hep-ph/0506176]; C. S. Chen, C. Q. Geng and D. V. Zhuridov, "Same-sign single dilepton productions at the LHC," arXiv:0801.2011 [hep-ph].

[32] M. Muhlleitner and M. Spira, "A note on doubly-charged Higgs pair production at hadron colliders," Phys. Rev. D **68**, 117701 (2003) [arXiv:hep-ph/0305288].

[33] CMS TDR: *CMS Physics: Technical Design Report V.2: Physics Performance*, CERN-LHCC-2006-021.

[34] ATLAS TDR: *ATLAS detector and physics performance. Technical design report. Vol. 2*, CERN-LHCC-99-15.